COMPARATIVE ANALYSIS IN TERMS OF PAPR AND PSD CONSIDERING VARIOUS FILTERS IN FBMC.

A Project report submitted in partial fulfillment of the requirements for the award of the degree of

BACHELOR OF TECHNOLOGY
IN
ELECTRONICS AND COMMUNICATION ENGINEERING

Submitted by

N. Chandra Sekhar (317126512040) G. Sai Ganesh (317126512021)

V. Varshith (317126512058) S. Meghna (317126512038)

Under the guidance of
Dr. A. Lakshmi Narayana
Assistant Professor

DEPARTMENT OF ELECTRONICS AND COMMUNICATION ENGINEERING
ANIL NEERUKONDA INSTITUTE OF TECHNOLOGY AND SCIENCES
(UGC AUTONOMOUS)
(*Permanently Affiliated to AU, Approved by AICTE and Accredited by NBA & NAAC with 'A' Grade*)
Sangivalasa, bheemili mandal, visakhapatnam dist. (A.P) 2020-2021

DEPARTMENT OF ELECTRONICS AND COMMUNICATION ENGINEERING
ANIL NEERUKONDA INSTITUTE OF TECHNOLOGY AND SCIENCES
(UGC AUTONOMOUS)
(Permanently Affiliated to AU, Approved by AICTE and Accredited by NBA & NAAC with 'A' Grade)
Sangivalasa, Bheemili mandal, Visakhapatnam dist. (A.P)

ANITS

CERTIFICATE

This is to certify that the project report entitled **"COMPARATIVE ANALYSIS IN TERMS OF PAPR AND PSD CONSIDERING VARIOUS FILTERS IN FBMC".** submitted by N. Chandra Sekhar (317126512040), G. Sai Ganesh (317126512021), V. Varshith (317126512058), S. Meghna (317126512038) in partial fulfillment of the requirements for the award of the degree of **Bachelor of Technology** in **Electronics & Communication Engineering** of Andhra University, Visakhapatnam is a record of bonafide work carried out under my guidance and supervision.

Project Guide
Dr. A. Lakshmi Narayana
Assistant Professor
ANITS

Assistant Professor
Department of E.C.E.
Anil Neerukonda
Institute of Technology & Sciences
Sangivalasa, Visakhapatnam-531 162

Head of the Department
Dr. V. Rajya Lakshmi
Professor & HOD
Department of E.C.E
ANITS

Head of the Department
Department of E C E
Anil Neerukonda Institute of Technology & Sciences
Sangivalasa - 531 162

ACKNOWLEDGEMENT

We would like to express our deep gratitude to our project guide **Dr. A. Lakshmi Narayana** Assistant Professor, Department of Electronics and Communication Engineering, ANITS, for his guidance with unsurpassed knowledge and immense encouragement.

We are grateful to **Dr V. Rajya Lakshmi**, Head of the Department, Electronics and Communication Engineering, for providing us with the required facilities for the completion of the project work.

We are very much thankful to the **Principal and Management, ANITS, Sangivalasa,** for their encouragement and cooperation to carry out this work.

We express our thanks to all **teaching faculty** of Department of ECE, whose suggestions during reviews helped us in accomplishment of our project. We would like to thank **all non-teaching staff** of the Department of ECE, ANITS for providing great assistance in accomplishment of our project.

We would like to thank our parents, friends, and classmates for their encouragement throughout our project period. At last but not the least, we thank everyone for supporting us directly or indirectly in completing this project successfully.

PROJECT STUDENTS

N. Chandra Sekhar (317126512040)

G. Sai Ganesh (317126512021)

V. Varshith (317126512058)

S. Meghna (317126512038)

ABSTRACT:

In this project, In future generation, the data consumption will be increased and in current technologies like 3G and 4G cannot handle the large data rate so 5G (fifth generation) is required. we are using a filter bank multi-carrier (FBMC) for 5G communication that will reduces the problems in 4G (orthogonal frequency division multiplexing-OFDM). In 4G we use cyclic prefix (CP) that requires high power to maintain it, so in 5G we are using banks of filter i.e.., FBMC. This FBMC technique used in 5G for high data rate in cellular and wireless systems. We use prototype filter response called PHYDYAS (physical layer for dynamic spectrum access and cognitive radio) in 5G communication.

This project shows the comparison of power spectral density (PSD) and PAPR for OFDM and FBMC. A sidelobe power of -70 dB is reduced in FBMC compared to OFDM is observed, PSD of FBMC using different filter and PAPR of OFDM and FBMC are also shown in this project.

CONTENTS

LIST FIGURES

PAGE NO

LIST OF ABBREVATIONS

ABBREVATIONS	DESCRIPTIONS
FBMC	Filter bank multicarrier
OFDM	Orthogonal frequency division multiplexing
CDMA	Code division multiple access
CP	Cyclic prefix
FFT	Fast Fourier Transform
IFFT	Inverse Fast Fourier Transform
QAM	Quadrature amplitude modulation
OQAM	Offset Quadrature amplitude modulation
BER	Bit error rate
PSD	Power spectral density
SNR	Signal to Noise ratio
PAPR	Peak to average power ratio
DFT	Discrete Fourier Transform
IDFT	Inverse Discrete Fourier Transform
ISI	Inter symbol interference
PPN	Poly phase network
CMF	Cosine modulated multitone
MIMO	Multiple input multiple output

CHAPTER 1

INTRODUCTION

1.1 OVERVIEW:

The world of mobile communication technology is a revolutionary paradigm shift, undergoing extensive transformations and widely used to connect people around the world. Mobile communication technology has made it possible for people to connect and communicate in remote parts of the world where even electricity cannot be taken for granted [1]. Mobile communication technologies developed from supporting analog voice only to powerful systems that provided countless of different applications to billions of consumers [2]. Figure 1.1 shows the timeline of various networking communication technologies categorized into 'Generations' [3]. Subsequently, the digital wireless communication systems are consistently on a delegation to achieve the growing need of human beings.

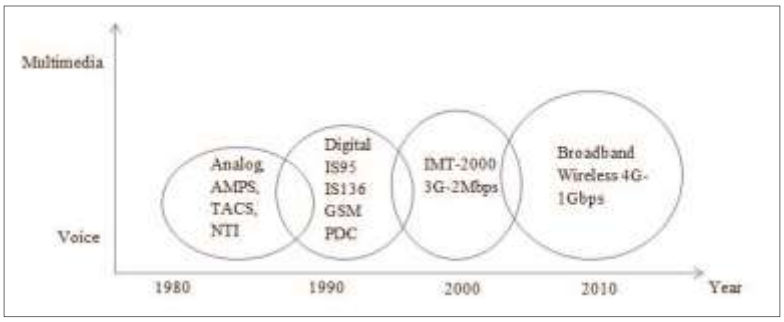

FIGURE 1.1 Evolution of Mobile Networks

First Generation (1G) was introduced in 1980s and provided voice transmissions and bandwidth of 2kbps [4]. 1G is an analog system and comprised of the following technologies which are Advance Mobile Telephone Systems (AMTS), Improved Mobile Telephone Service (IMTS), Push to Talk (PTT) and Mobile Telephone System (MTS) [3]. Second Generation (2G) started in 1990s and was commercially launched on the GSM standard which based on digital technology and network infrastructure with the speed up to 14.4kbps. 2G consist of the

following technologies which are Global System for Mobile Communication (GSM), Enhanced Data Rates for GSM Evolution (EDGE), Code Division Multiple Access (CDMA) and General Packet Radio Service (GPRS) [3]. Third Generation (3G) introduced in 2000s quest for data at higher speeds [4]. It substantiates video calling with the speed up to 2Mbps. 3G comprises of Universal Mobile Telecommunication Systems (UMTS), Wideband CDMA, UBluetooth, High Speed Downlink Packet Access (HSDPA) and Wireless Local Area Network (WLAN) [3].

Fourth Generation (4G) introduced in 2000s. 4G uses the concept of connectivity anywhere, anytime from any kind of devices and it is indeed observed in user behavior [5]. It supposed to provide 100Mbps to 1Gbps to users [6] and the range of latency between 40ms and 60ms. 4G able to delivering faster and better mobile broadband experiences besides application of mobile web access and the high quality of videos and images. Besides that, 4G LTE were introduced because it is not able to fully reach the range of 4G. The download process, stream and browse faster with better connectivity. It is closer to meet the criteria of standards. Next, LTE-Advanced was introduced which is more progressive of technologies and standards which is capable to deliver faster and bigger data. Besides that, it offers to deliver true speeds of 4G compared to the LTE networks. 4G comprised Long Term Evolution (LTE), Worldwide Interoperability for Microwave Access (WiMAX), Multiple Input Multiple Output (MIMO) smart antenna technologies, Mobile Broadband Wireless Access (MBWA) and Orthogonal Frequency Division Multiplexing (OFDM). Nowadays, there are more powerful laptops and smartphones which is becoming more attractive and demanding advanced multimedia capabilities. This has led to an eruption of wireless mobile devices and services.

1.2 FUTURE 5G MOBILE COMMUNICATION TECHNOLOGY

The exciting growth of smartphones, laptops, devices that connected with the wireless systems, coupled with improved applications are expected to use up the extra capacity from higher spectral efficiency and additional spectrum of 4G mobile communication system [8]. The future fifth generation (5G) mobile communication technology will be implemented

with 100-100Mbps user data rate, 20Gbps peak data rate and the reduction of latency time until 1ms. It provides better coverage and speed facility to users besides become huge demand in future. This technology will generate an ultrahigh speed which is possible to change the meaning of cell phone usability. The significant appearances that will fascinated people is the connectivity with low latency, more gaming options and comprehensive multimedia options with high quality audio and video.

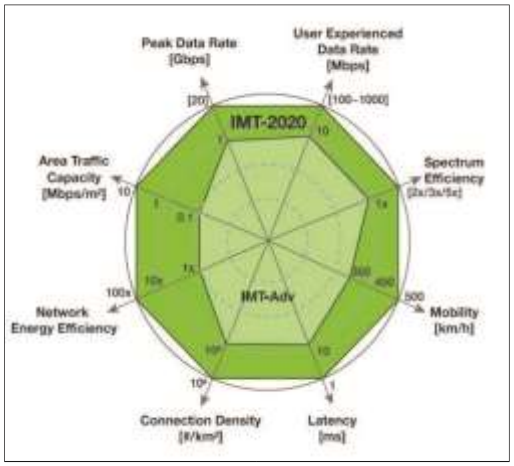

FIGURE 1.2 The requirements of 5G mobile communication technology

5G mobile communication technology attracted worldwide research attention in the recent years with the vision to have 100 billion connections, close to zero latency which is low latency and 1000 times throughput enhancement. 5G is high reliability and throughput, increase scalability an energy efficient and low latency [9]. To achieve the requirements, it needs to figure out the physical layer of the modulation and coding up to all the routing schemes and network topology [10]. Figure 1.2 shows the requirements of future 5G mobile communication technology. This technology will be introduced beyond 2020 and expected to support a new frequency bands with the wider spectral bandwidth per frequency channel. The predecessor of this technologies have proved substantial increase in peak bit rate and rather 5G is also advanced in connectivity concurrently and instantaneously, high capacity to allow more devices, larger data volume per unit area, higher reliability of the communication and lower battery consumptions. 5G technology includes all types of advanced technology which make this system becomes powerful in massive demand besides provides the mobile phone consumers more efficiency and features.

5G is a packet switched wireless system with expanded area coverage and high throughput.

This technology will be used millimeter wireless and Code Division Multiple Access (CDMA) that enables speed higher than 1Gbps at low mobility and greater than 100Mbps at full mobility. 5G technology offered high resolution for extreme mobile consumers, higher data rates, bidirectional huge bandwidth and the finest Quality of Service (QoS). 5G technology will be supported the connections for at least 100 billion devices with low latency and 10Gbps throughput. Figure 3 shows the research directions in future 5G mobile communication technology.

CHAPTER 2
FILTER BANK MULTICARRIER (FBMC)

2.1 FILTER BANK MULTICARRIER (FBMC)

There are several ideas for future 5G mobile communication technology that could bring additional advantages to the new cellular system such as FBMC, filtered OFDM (f-OFDM), Generalized Frequency Division Multiplexing (GFDM) and Universal Filtered Multicarrier (UFMC) are now still under research. However, this paper focused on OFDM and FBMC technique. Multicarrier modulation becomes an important technique over the past several years for the realization of broadband communication technology [5] besides, recognize as an efficient scheme for wideband transmission [1]. FBMC is a combination of multiplexing and modulation with function by breaking the wideband channel into a number of narrowband channels which is called the subchannels. The complicated modulation values of FBMC systems will be spread over several carriers and filtered by a prototype filter [1].

The simple concept and low complexity in OFDM systems makes the FBMC systems received a limited attention. The FBMC system offers more robustness to the time and frequency offset than OFDM and does not use any Cyclic Prefix (CP) extension [14]. In the FBMC system, the signal with high spectral containment will be used to reduce the sidelobes of each subcarrier frequency. Figure 2.1 shows the frequency response for FBMC technique.

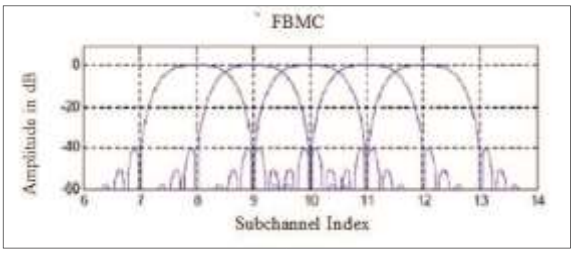

FIGURE 2.1 Frequency response for FBMC technique [13]

FBMC systems are a subclass of Multicarrier (MC) systems. FBMC modulation is a multicarrier modulation method in which a set of synthesis and analysis filters are employed at the transmitter and receiver respectively [7,8]. The filters uses in the FBMC systems are a set of bandpass filters. In this filter, the frequency shifted or modulated versions of a prototype lowpass filter. FBMC offers a better spectral containment than OFDM as the filter bandwidth, so the selectivity is a parameter that can be assorted during lowpass prototype design [1,2]. Besides that, FBMC gives the better bandwidth efficiency compared to OFDM. This is because, FBMC does not use the CP extension, so it will be attenuated the interferences within and close to the used frequency band efficiently. Next, the FBMC systems are comparatively more resistant to narrowband noise effects [20].

Figure 2.2 shows the graphical illustration of the FBMC transmitter meanwhile Fig. 2.3 shows the graphical illustration of a generic FBMC receiver. At the transmitter as shown in Fig. 6, the high speed input signal will be demultiplexed into N branches. After that, it will be modulated by the different or same signal constellation as required. The subsequent modulated branches are the upsampled to give N copies. The upsampled data will be sent through the set of synthesis filters gk(n),k=0,1,….,N-1. Next, to produce the transmitted signal s(n), the output of all filters will be summed together. At the receiver as shown in Fig. 7, to give N subcarriers of different center frequencies, the received signal r(n) will be passed through to the bank of analysis filters fk(n),k=0,1,….,N-1. The signal in every branch will be down sampled by N, demodulated and multiplexed to produce the estimate of the original signal Xr(n) [2].

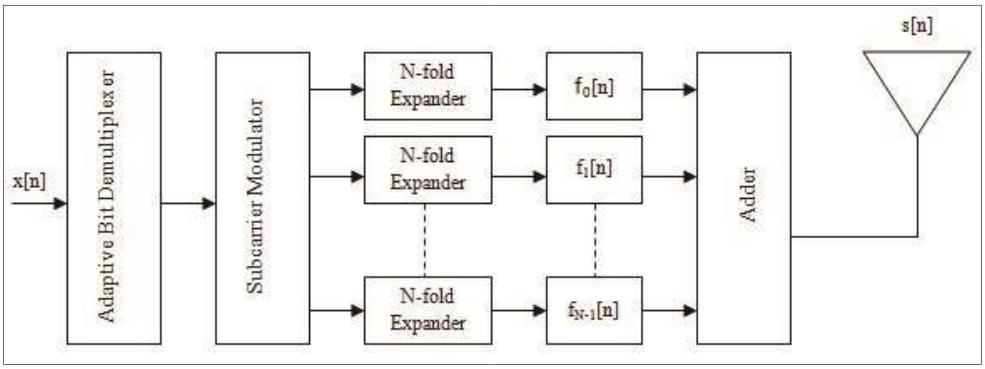

FIGURE 2.2 The graphical illustration of the FBMC transmitter

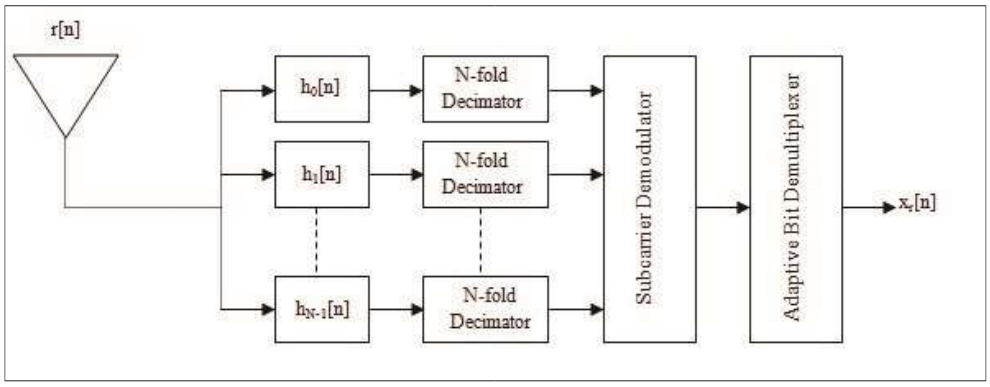

FIGURE 2.3 The graphical illustration of a generic FBMC receiver

MULTICARRIER MODULATION

The multicarrier modulation was considered as an effective way to attain high data rate transmission. This is because the total channel bandwidth was divided into sub-channels with subcarriers will be modulated with a lower data rate. The OFDM system band modulation is a special case of multicarrier transmission. The original data streams at lower data rates will be modulated separately in this system. Conventional modulation schemes are Quadrature Amplitude Modulation (QAM) of Phase Shift Keying (PSK). To achieve high speed data transmission, these lower data streams will be transmitted simultaneously through the subcarriers after modulation [2].

2.2 ORTHOGONAL FREQUENCY DIVISION MULTIPLEXING (OFDM)

Orthogonal Frequency Division Multiplexing (OFDM) is one of the modulation type used for current wireless and telecommunications systems. This system used the technique of encoding digital data on multiple carrier frequency and becomes a popular method for wideband digital communication. It is widely used to produce high data rates and

combating multipath fading in wireless communication technology. OFDM is already used over the world to attain high data rates which is needed for data intensive applications. It has been used in wireless network, audio broadcasting and 4G mobile communication technology.

This modulation format already been used in the WiFi arena (802.11a, 802.11ac, etc). OFDM use the Cyclic Prefix (CP) which will reduce the overall spectral efficiency [1]. OFDM based on the idea of modulating each data stream on subcarriers and dividing high-bit-rate data stream into several lower bit-rate data. Conventional OFDM makes use of Fast Fourier Transform (FFT) as its basic block [11]. Multicarrier modulation knowing as schemes which able to provide high data rate.

Figure 2.4 shows the frequency response for OFDM which exhibits strong sidelobes due to rectangular windowing [3]. OFDM is a wideband modulation technique which is able to handle with the issues of the multipath reception by transmitting many narrowband overlapping digital signals in parallel in one wide band. It is very useful for communication over channels with frequency selective fading. Nevertheless, it is difficult in handling selective fading in the receiver because of the complicate architecture of the receiver. Besides that, flat fading is easy to combat compared to the frequency selective fading by the use of simple error correction and equalization schemes [12].

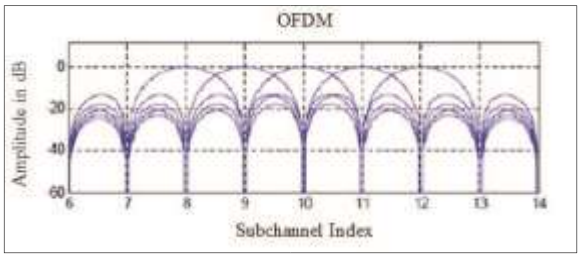

FIGURE 2.4 Frequency response for OFDM [13]

2.3 Review of FBMC Methods

FBMC communication techniques were first developed in the mid-1960s. Chang [3] presented the conditions required for signaling a parallel set of PAM symbol sequences through a bank of overlapping filters within a minimum bandwidth. To transmit PAM symbols in a bandwidth-efficient manner, Chang proposed vestigial sideband (VSB) signaling for subcarrier sequences. Saltzberg [4] extended the idea and showed how Chang's method could be modified for transmission of QAM symbols in a double-

sideband- (DSB-) modulated format. In order to keep the bandwidth efficiency of this method similar to that of Chang's signaling, Saltzberg noted that the in-phase and quadrature components of each QAM symbol should be time staggered by half a symbol interval. Efficient digital implementation of Saltzberg's multicarrier system through polyphase structures was first introduced by Bellanger and Daguet [1] and later studied by Hirosaki [3, 4]. Another key development appeared in [4], where the authors noted that Chang's/Saltzberg's method could be adopted to match channel variations in doubly dispersive channels and, hence, minimize intersymbol interference (ISI) and intercarrier interference (ICI). Saltzberg's method has received a broad attention in the literature and has been given different names. Most authors have used the name offset QAM (OQAM) to reflect the fact that the in-phase and quadrature components are transmitted with a time offset with respect to each other. Moreover, to emphasize the multicarrier feature of the method, the suffix OFDM has been added, hence, the name OQAM-OFDM

Chang's method [3], on the other hand, has received very limited attention. Those who have cited [9] have only acknowledged its existence without presenting much detail, for example [4, 5, 6]. In particular, Hirosaki who has extensively studied and developed digital structures for the implementation of Saltzberg's method [4, 7] has made a brief reference to Chang's method and noted that since it uses VSB modulation, and thus its implementation requires a Hilbert transformation, it is more complex to implement than Saltzberg's method. This statement is inaccurate, since as we have demonstrated in [8] Chang's and Saltzberg's methods are equivalent and, thus, with a minor modification, an implementation for one can be applied to the other. Also, as noted earlier, a vast literature in digital signal processing has studied a class of multicarrier systems that has been referred to as DWMT. It was later noted in [7, 8] that DWMT uses the same analysis and synthesis filter banks as the cosine modulated filter banks (CMFB) [9]. CMFB, on the other hand, may be viewed as a reinvention of Chang's method, with a very different application in mind [8]. In [8], we also introduced the shorter name cosine modulated multitone (CMT) to be replaced for DWMT and/or CMFB.

One more interesting observation is that another class of filter banks which were called modified DFT (MDFT) filter bank has appeared in the literature [5]. Careful study of MDFT reveals that this, although derived independently, is in effect a reformulation of Saltzberg's filter bank in discretetime and with emphasis on compression/coding. The literature on MDFT begins with the pioneering works of Fliege [5] and later has been extended by others, for example [5–8].

Finally, before we proceed with the rest of our presentation, it should be reiterated that we identified three types of FBMC systems: (i) CMT: built based on the original idea of Chang [9]; (ii) SMT: built based on the extension made by Saltzberg [4]; and (iii) FMT: built based on the conventional method frequency division multiplexing (FDM)

2.4 Theory

The theory of FBMC, particularly those of CMT and SMT, has evolved over the past five decades by many researchers who have studied them from different angles. Early studies by Chang [9] and Saltzberg [4] have presented their finding in terms of continuous-time signals. The more recent studies have presented the formulations and conditions for ISI and ICI cancellation in discrete-time, for example, [6, 5]. On the other hand, a couple of recent works [1, 8], from the author of this paper and his group, have revisited the more classical approach and presented the theory of CMT and SMT in continuous time. It is believed that this formulation greatly simplifies the essence of the theoretical concepts behind the theory of CMT and SMT and how these two waveforms are related. It also facilitates the design of prototype filters that are used for realization of CMT and SMT systems. Thus, here, also, we follow the continuous-time approach of [3, 8].

mostly through the *time-frequency phase-space*, with minimum involvement in mathematical details. It is believed that this presentation also provides a new intuition into the relationship between SMT and CMT. Interested readers who wish to see the mathematical details are referred to [2, 8].

2.4.1 CMT.

In CMT, data symbols are from a pulse amplitude modulated (PAM) alphabet and, hence, are real-valued. To establish a transmission with the maximum bandwidth efficiency, PAM symbols are distributed in a time-frequency phase-space lattice with a density of two symbols per unit area. This is equivalent to one complex symbol per unit area. Moreover, because of the reasons that are explained below a 90-degree phase shift is introduced to the respective carriers among the adjacent symbols. These concepts are presented in Figure 2.5 Vestigial side-band (VSB) modulation is applied to cope with the carrier spacing $F = 1/2T$. The pulse-shape used for this purpose at the transmitter as well as for matched filtering at the receiver is a square-root Nyquist waveform

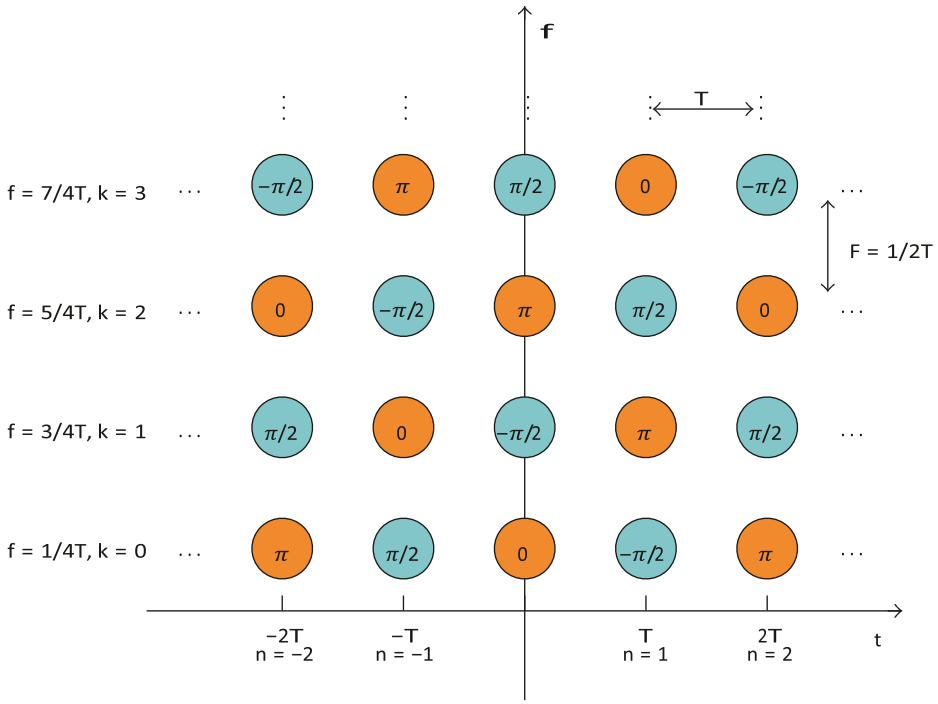

Figure 2.5 The CMT time-frequency phase-space lattice.

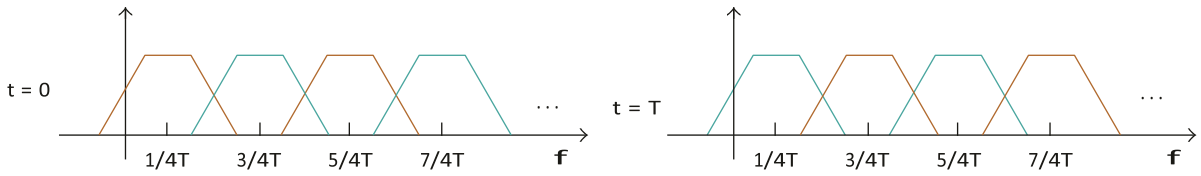

(a) (b)

Figure 2.6 Magnitude responses of the CMT pulse-shaping filters at various subcarriers and time instants $t = 0$ and $t = T$.

Moreover, to give a complement presentation to those of [8, 11], an attempt is made to discuss the underlying theory mostly through the *time-frequency phase-space*, with minimum involvement in mathematical details. It is believed that this presentation also provides a new intuition into the relationship between SMT and CMT. Interested readers who wish to see the mathematical details are referred to [2, 8].

$p(t)$, which has been designed such that$q(t) = p(t) \star p(-t)$ is a Nyquist pulse with regular zero crossings at 2T time intervals.

Also, $p(t)$, by design, is a real-valued function of time and $p(t)=p(-t)$. These properties of $p(t)$, as demonstrated below, are instrumental for correct functionality of CMT.

Figure 2.6 presents a set of magnitude responses of the modulated versions of the pulse-shape $p(t)$ for the data symbols transmitted at t=0 and t=T. The colors used for the plots follow those in Figure 1 to reflect the respective phase shifts.

Let n= …,-2,-1,0,1,2,… , denote symbol time index, let k=0,1,2,… , denote symbol frequency index $s_k[n]$, let denote the (n, k) data symbol in the time-frequency lattice, and let $\theta k[n] = (k - n)(\pi/2)$ be the phase shift that is added to the carrier of $s_k[n]$. Accordingly, a CMT waveform that is constructed based on the pulse-shape/prototype filter $p(t)$ is expressed as

$$x(t) = \sum_n \sum_k s_k[n] a_{n,k}(t) \qquad \text{- (1)}$$

Where,

$$a_{n,k}(t) = e^{j\theta_k[n]} P_{n,k}(t)$$

$$P_{n,k}(t) = p(t - nT) e^{j\left((2K+1)\pi/2T\right)t}$$

The synthesis of $x(t)$ according to (1) has the following interpretations. The terms $a_{n,k}(t)$ may be thought as a set of basis functions that are used to modulate the data symbols $s_k[n]$. The data symbols $s_k[n]$ can be extracted from x(t) straightforwardly if $a_{n,k}(t)$ are a set of orthogonal basis functions. The orthogonality for a pair of functions $V_1(t)$ and

$V_2(t)$, in general, is defined as

$$< v_1(t), v_2(t) >= \int_{-\infty}^{\infty} v_1(t) v_2^*(t)\, dt = 0 \qquad \text{-- (2)}$$

For the case of interest here, where the data symbols $s_k[n]$ are real-valued, the orthogonality definition (3) can be replaced by the more relaxed definition:

$$< v_1(t), v_2(t) >= \boldsymbol{R}\{ \int_{-\infty}^{\infty} \boldsymbol{v_1(t) v_2^*(t)\, dt} \} = \mathbf{0} \quad \text{-- (3)}$$

where R{.} indicates the real part. Definition (4) is referred to as *real orthogonality*.

It is not difficult to show that

$$< a_{n,k^{(t)},a_{m,l}}(t) >_R = \begin{cases} 1, & n = m, k = l \\ 0, & \text{otherwise} \end{cases} \qquad \text{-}$$

-(4)

and, hence, for any pair of n and k,

$$s_k[n] =< x(t), a_{\eta,k}(t) >_R \qquad \text{--(5)}$$

To develop an in-depth understanding of the CMT signaling, it is instructive to explore a detailed derivation of

(5). To this end, we begin with the definition

$$< a_{n,k^{(t)},a_{m,l}}(t) >_R = R\{\int_{-\infty}^{\infty} 1.\, e^{j\theta_k[\eta]}\, P_{n,k}(t) e^{-j\theta_1[m]}\, P_{m,l}^*(t) dt \quad \text{--(6)}$$

and note that this can be rearranged as

$$< a_{n,k^{(t)},a_{m,l}}(t) >_R = R\{\int_{-\infty}^{\infty} 1.e^{j(m-n+k-l)\left(\frac{\pi}{2}\right)} p(t-nT) \times p(t-nT))e^{j((k-l)(\frac{\pi}{T}))t} dt\}$$

--(7)

When m=n and k=l, after a change of variable t to t+nt,

$$\langle a_{n,k}(t), a_{n,k}(t)\rangle_R = \int_{-\infty}^{\infty} p^2(t)\,dt = 1,$$

-- (8)

where the second equality follows from the fact that $p(t)$ is a real-valued square-root Nyquist pulse and $p(t)=p(-t)$.

When $k = l$, $m \neq n$, and $m - n = 2r$, where r is an integer

$$< a_{n,k^{(t)},a_{m,l}}(t) >_R = (-1)^r \int_{-\infty}^{\infty} p(t-nT)p(t-mT)\,dt = 0$$

- (9)

where the second equality follows since $p(t)$ is a square root Nyquist pulse, designed for a symbol spacing 2T.On the other hand, when $k = l$, but $m - n = 2r + 1$,

$$< a_{n,k^{(t)},a_{m,l}}(t) >_R = R\{ j(-1)^r \int_{-\infty}^{\infty} p(t-nT)p(t-mT)\,dt\}=0$$

--(10)

Next, consider the case where k-l=1 and m-n=2r. In that case, one finds that

$$\begin{aligned}\langle a_{n,k}(t), a_{m,l}(t)\rangle_R &= \Re\left\{ j(-1)^r \int_{-\infty}^{\infty} p(t-nT)\, p(t-mT)\, e^{j(\pi/T)t} dt\right\} \\ &= -(-1)^r \int_{-\infty}^{\infty} p(t-nT)\, p(t-mT) \sin\left(\frac{\pi}{T}t\right) dt \\ &= 0,\end{aligned}$$

-- (11)

where the last identity follows, by applying the change of

variable $t \rightarrow t + ((m + n)/2)T$ and noting that the expression under the integral will reduce to an odd function of t. Following similar procedures, it can be shown that the

real orthogonality $\langle an,k(t), am,l(t)\rangle R= 0$ also holds, when k-l=1 and m-n is an odd integer, and when k-l=-1 and m-n is either an even or odd integer. Finally, for the cases where $|k - l|_{>1}$, the real orthogonality $\langle an,k(t), am,l(t)\rangle R= 0$ is trivially confirmed by noting that the underlying basis functions correspond to filters that have no overlapping bands. The stop-band quality of the frequency response of the prototype filter $p(t)$ determines the accuracy of the equality $\langle an,k(t), am,l(t)\rangle R= 0$ when $|k - l| > 1$.

It is also worth noting that some of the recent derivations of FBMC that are presented in discrete-time design the respective prototype filter $p[n]$ such that the respective real orthogonality is perfectly satisfied for the cases where $|k - l|>1$ as well, for example, [6]. However, one may realize that, in practice, the presence of channel destroys the orthogonality of the basis functions. The orthogonality of the basis functions is commonly recovered at the receiver using per subcarrier equalizers; see Section 6, below. Such equalizers, unfortunately, will not be able to recover the orthogonality of basis functions that belong to nonadjacent subcarriers. Hence, the design of a $p[n]$ that satisfies the real orthogonality for $|k - l|>1$ may be a waste.

To summarize, the above derivations revealed that the following settings of the CMT parameters lead to the real orthogonality of the basis functions $a_{n,k}(t)$ and allow symbol placement in the time-frequency lattice at the maximum density of two real symbols per unit area.

(1) The symbol spacing T along the time axis should be matched with the subcarrier spacing $F = 1/2T$ along the frequency axis.

The pulse-shape/prototype filter $p(t)$ must be a realvalued square-root Nyquist filter for a symbol spacing

2_T. It should be also a linear phase; hence, when viewed as a zero phase filter, it satisfies the condition

$p(t)=p(-t)$. The latter is not a necessary condition but is satisfied in most of the designs; see [38] for a more relaxed condition.

(2) The above constraints are applied to assure orthogonality of the basis functions that are within the same subcarrier or adjacent subcarriers only. The orthogonality of basis functions that belong to the nonadjacent subcarriers is guaranteed by virtue of the fact that they correspond to filters with nonoverlapping bands. A more advanced design presented in Section 4.2 allows overlapping of the nonadjacent bands and yet satisfies the orthogonality condition. (4) The phase shifts indicated in Figure 1 can be modified to other choices, as long as a phase difference $\pm_{\pi/2}$ is preserved between each pair of adjacent points in the lattice.

(3) Although in CMT the position of the lattice points is fixed, these points can be moved in the time frequency plane as long as their relative position and phase differences remain unchanged. We usethis point below to arrive at the SMT waveform by applying a simple modification to the CMT waveform

The below equations may be combined to arrive at the CMT transmitter and receiver structures that are presented in Figure 2.7 As shown a synthesis filter bank (SFB) is used to construct the transmit signal, and the received signal is passed through an analysis filter bank (AFB) to separate the data streams of different subcarrier bands. Here, it is assumed that there are N subcarrier streams and the data stream of the kth subcarrier at the input to the SFB is represented by the impulse train:

$$s_k(t) = \sum_n s_k[n]\,\delta(t - nT)\,.$$

-- (12)

It is also worth noting that, in practice, the analyzed signals at the output of the AFB should be equalized. Here, to keep the presentation simple, we have not included the equalizers.

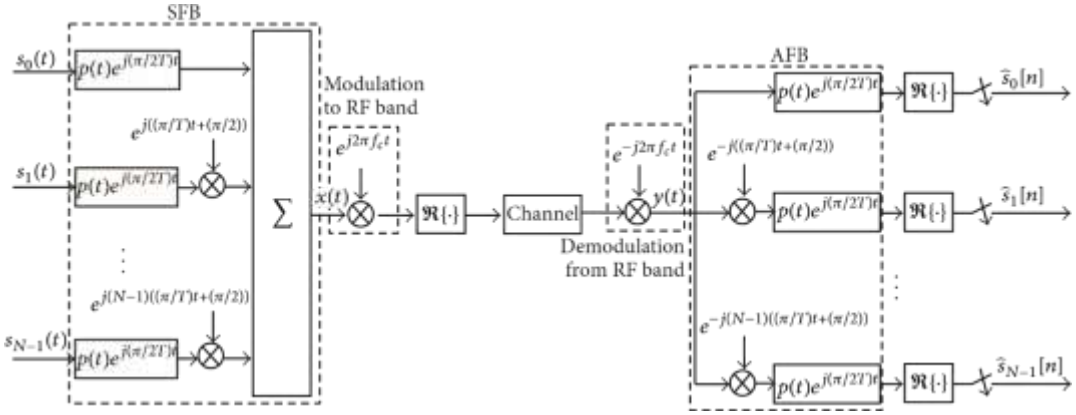

Figure 2.7 CMT transmitter and receiver blocks.

2.4.2 SMT

SMT may be thought of as an alternative to CMT. Its time-frequency phase-space lattice is obtained from that of CMT (Figure 1) through a frequency shift of the lattice points down by ¼ T, scaling the time axis by a factor ½ and hence the frequency axis by a factor 2. Moreover, to remain consistent with the past literature of SMT (equivalently, OQAM-OFDM), some adjustments to the carrier phases of the lattice points have been made. This leads to the time frequency phase-space lattice that is presented in Figure 2.8 The magnitude responses of the SMT pulse-shaping filters at various subcarriers and time instants t=0 and t=T/2 are presented in Figure 2.9 Note that here the PAM symbols are spaced by $T/2$ and subcarriers are spaced by 1/T. In SMT, each pair of adjacent symbols along time in each subcarrier is treated as real and imaginary parts of a QAM symbol. Its in-phase and quadrature components as $s_k[n]= s_k^I[n]+ j s_k^Q[n]$. Accordingly, the inputs to the SFB

$$s_k^I(t) = \sum_n s_k^I[n]\,\delta(t - nT),$$

$$s_k^Q(t) = \sum_n s_k^Q[n]\,\delta(t - nT).$$

--(13)

...

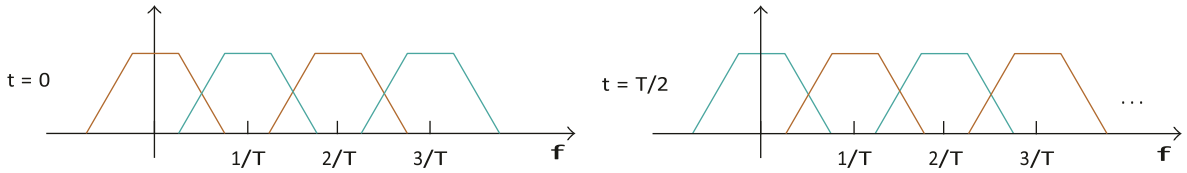

Figure 2.8 The SMT time-frequency phase-space lattice.

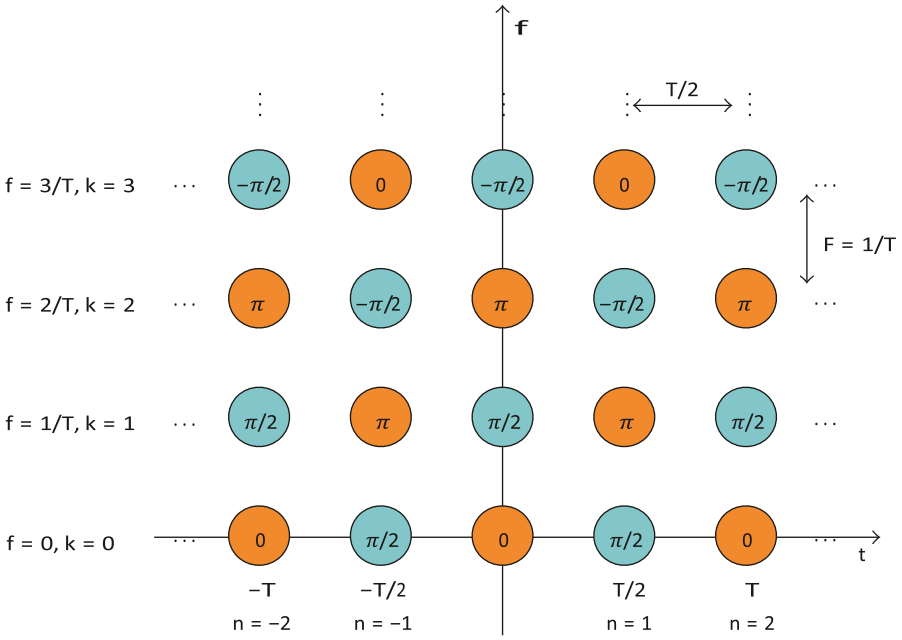

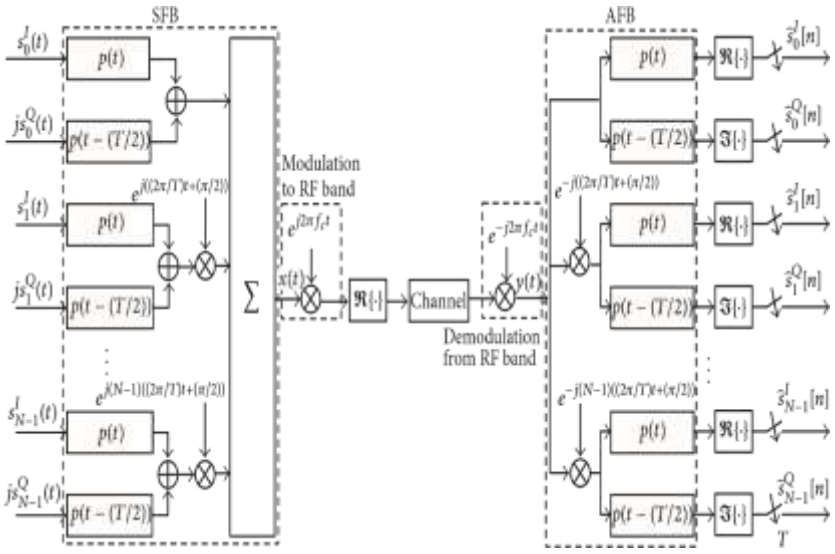

Figure 2.9 SMT transmitter and receiver blocks.

FMT. FMT waveforms are synthesized following the conventional method of frequency division multiplexing (FDM). The subcarrier channels have no overlap, and thus ICI is resolved through use of well-designed filters with high stopband attenuation. ISI may be compensated for by adopting the conventional method of square-root Nyquist filtering that is used in single-carrier communications. For doubly dispersive channels, we have adopted a more advanced design [7] that compensates for both ICI and ISI For comparison with the CMT and SMT structures in Figures 2.7 and 2.9, respectively, and also as a basis for further development in later parts of this paper, Figure presents the structures of transmitter and receiver blocks in an FMT communication system. Also, the magnitude responses of the FMT pulse shaping filters at various sub carriers are presented in Figure 2.11 Note that here the subcarrier spacing is equal to $(1 + \alpha)/T$, where α is the roll-off factor of the pulse

shaping/prototype filter. Accordingly, FMT has a symbol density of $1/(1+\alpha)$ complex symbols per unit area in the time frequency plane. Hence, FMT is less bandwidth efficient than CMT and SMT.

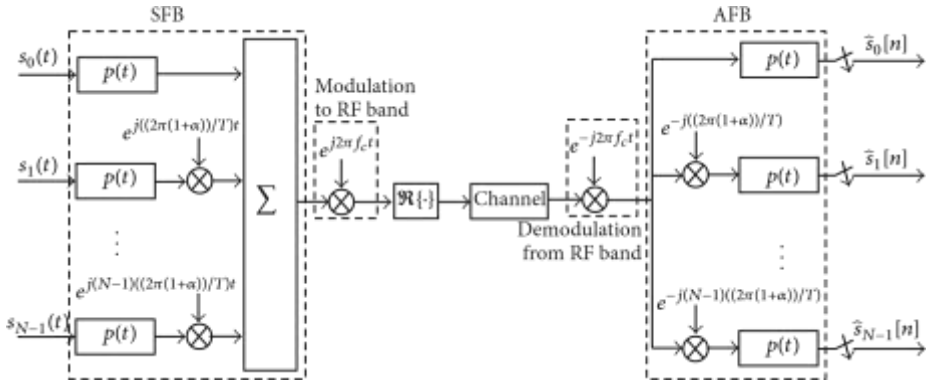

Figure 2.10 FMT transmitter and receiver

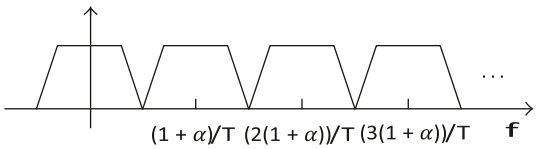

Figure 2.11 Magnitude responses of an FMT pulse-shaping filter at various subcarriers.

CHAPTER 3
FILTER DESIGN

3.1 The FFT as Multicarrier Modulator:

The inverse fast Fourier transform (IFFT) can serve as a multicarrier modulator and the fast Fourier transform (FFT) can serve as a multicarrier demodulator. A multicarrier transmission system is obtained and the transmitter and the receiver are shown in Fig.3.1.

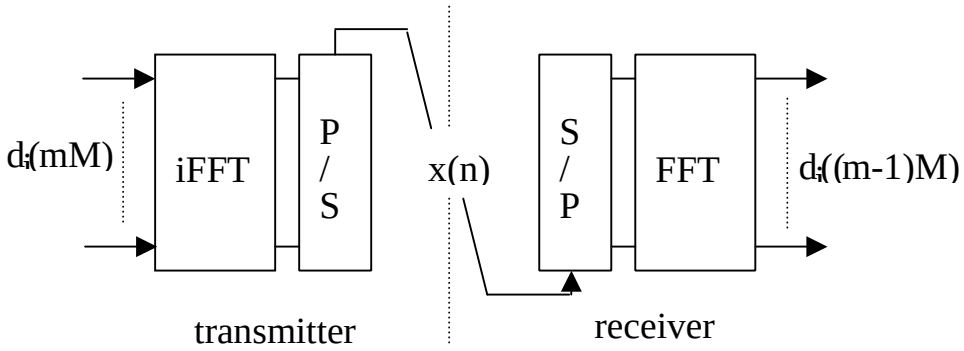

Fig.3.1 Multicarrier modulation with the FFT

It is obvious from the figure that the block of data at the input of the iFFT in the transmitter is recovered at the output of the FFT in the receiver, since the FFT and the iFFT are cascaded. The detailed description of the operations is as follows. The size of the iFFT and the FFT is M and a set of M data samples, di(mM) with $0 \leq i \leq M-1$, is fed to the iFFT input. For $mM \leq n < (m+1)M$ the iFFT output is expressed by

$$X(n) = \sum_{i=0}^{M-1} d_i(mM) e^{j2\pi i(n-mM)/M} \quad \text{-- (14)}$$

The set of M samples so obtained is called a multicarrier symbol and m is the symbol index. For transmission in the channel, a parallel-to-serial (P/S) converter is introduced at the output of the iFFT and the samples x(n) appear in serial form. The sampling frequency of the transmitted signal is unity, there are M carriers and the carrier frequency spacing is 1/M. The duration of a multicarrier symbol T is the inverse of the carrier spacing, T=M. Note that T is also the multicarrier symbol period, which reflects the fact that successive multicarrier symbols do not overlap in the time domain. An illustration is given in Fig.3.2 for i = 2 and d2(mM) = ± 1. The

transmitted signal x(n) is a sine wave and the duration T contains i = 2 periods. Similarly, di(mM) is transmitted by i periods of a sine wave in the duration T . Overall, the

transmitted signal is a collection of sine waves such that the symbol duration contains an integer number of periods. In fact, it is the condition for data recovery, the so-called orthogonality condition. At the receive side, a serial-to-parallel (S/P) converter is introduced at the input of the FFT. The data samples are recovered by

$$d_i(mM) = 1/M \sum_{n=mM}^{mM+M-1} d_i(mM) e^{-j2\pi i(n-mM)/M} \quad \text{--(15)}$$

Note also in Fig.1 that, due to the cascade of P/S and S/P converters, there is a delay of one multicarrier symbol at the FFT output with respect to the iFFT input.

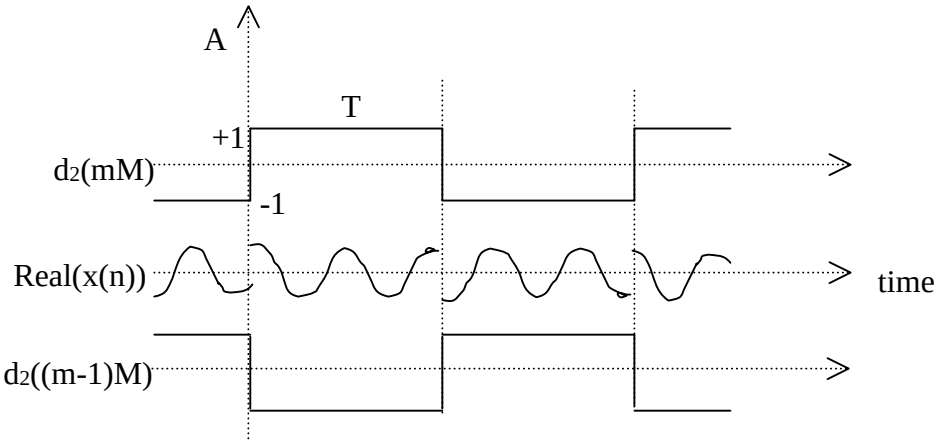

Fig.3.2 Data and transmitted signals

For the proper functioning of the system, the receiver (FFT) must be perfectly aligned in time with the transmitter (iFFT). Now, in the presence of a channel with multipath propagation, due to the channel impulse response, the multicarrier symbols overlap at the receiver input and it is no more possible to demodulate with just the FFT, because intersymbol interference has been introduced and the orthogonality property of the carriers has been lost.

Then, there are 2 options:

1) extend the symbol duration by a guard time exceeding the length of the channel impulse response and still demodulate with the same FFT. The scheme is called OFDM.

2) keep the timing and the symbol duration as they are, but add some processing to the FFT. The scheme is called FBMC, because this additional processing and the FFT together constitute a bank of filters. The present document is concerned with this second approach and, as an introduction, it will first be shown that the FFT itself is a filter bank.

Filtering effect of the FFT

Let us assume that the FFT is running at the rate of the serially transmitted samples. Considering Fig.3.1, the relationship between the input of the FFT and the output with index k = 0 is the following

$$y_0(n) = 1/M[\, x(n-M)+....+ x(n-1)] = 1/M\sum^{M}_{i=1}x(n-i) \quad \text{--(16)}$$

This is the equation of a low-pass linear phase FIR filter with the M coefficients equal to 1/ M . Disregarding the constant delay, the frequency response is

$$I(f) = \sin\pi f M / M \sin\pi f$$

It is shown in Fig.3.3, where the unit on the frequency axis is 1/M.

In the same conditions, the FFT output with index k is expressed by

$$y_k(n) = 1/M \sum_{i=0}^{M-1} x(n-M+i)e^{-j2\pi ki/M} \quad \text{--(17)}$$

Changing variables and replacing i by M− i , an alternative expression is

$$y_k(n) = 1/M \sum_{i=1}^{M} x(n-i)e^{j2\pi ki/M} \quad \text{--(18)}$$

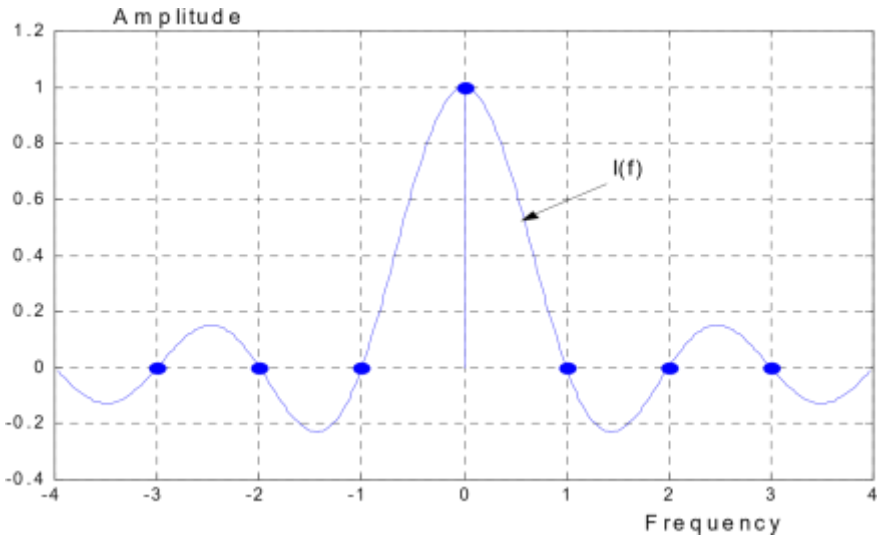

Fig.3.3. FFT filter frequency response and coefficients in the frequency domain

The filter coefficients are multiplied by $e^{j2\pi k/M}$, which corresponds to a shift in frequency by k / M of the frequency response. When all the FFT outputs are considered, a bank of M filters is obtained, as shown in Fig.3.4, in which the unit on the frequency axis is 1/ M , the sub-carrier spacing. The orthogonality condition appears through the zero crossings: at the frequencies which are integer multiples of 1/ M , only one filter frequency response is non-zero.

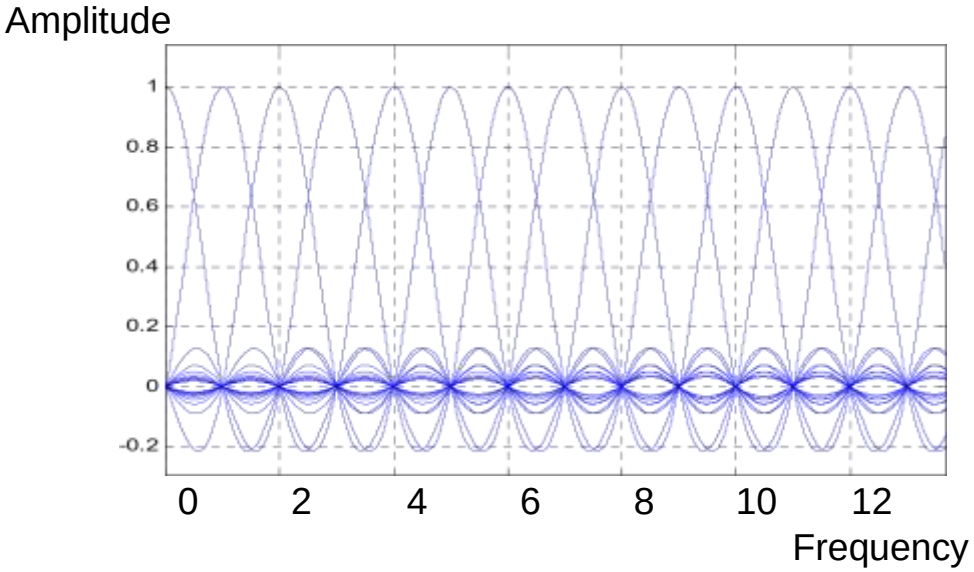

Fig.3.4. The FFT filter bank (frequency unit: sub-carrier spacing)

An FIR filter can be defined by coefficients in the time domain or by coefficients in the frequency domain. The two sets of coefficients are equivalent and related by the discrete Fourier transform (DFT). Returning to the first filter in the bank, the DFT of its impulse response consists of a single pulse, as shown in Fig.3.3. In fact, the frequency coefficients are the samples of the frequency response I(f), which, according to the sampling theory, is derived from them through the interpolation formula. In the terminology of filter banks, the first filter in the bank, the filter associated with the zero frequency carrier, is called the prototype filter, because the other filters are deduced from it through frequency shifts. It is clearly apparent in Fig.3.4 that I(f) is the frequency response of a prototype filter with limited performance, particularly out-of-band attenuation. In order to reduce the out-of-band ripples, it is necessary to increase the number of coefficients in the time domain and, equivalently, in the frequency domain. Then, in the time domain, the filter impulse response length exceeds the multicarrier symbol period T . In the frequency domain, additional coefficients are inserted between the existing coefficients, allowing for a better control of the filter frequency response. Prototype filters are characterised by the overlapping factor K, which is the ratio of the filter impulse response duration Θ to the multicarrier symbol period T . The factor K is also the number of multicarrier symbols which overlap in the time domain. Generally, K is an integer number and, in the frequency domain, it is the number of frequency coefficients which are introduced between the FFT filter coefficients. Now, the question is how to design the prototype filter and transmit data in such a manner that no intersymbol interference occurs, in spite of the overlapping.

3.2 Prototype filter design – Nyquist criterion

Digital transmission is based on the Nyquist theory: the impulse response of the transmission filter must cross the zero axis at all the integer multiples of the symbol period. The condition translates in the frequency domain by the symmetry condition about the cut-off frequency, which is half the symbol rate. Then, a straightforward method to design a Nyquist filter is to

consider the frequency coefficients and impose the symmetry condition. In transmission systems, the global Nyquist filter is generally split into two parts, a half-Nyquist filter in the transmitter and a half-Nyquist filter in the receiver. Then, the symmetry condition is satisfied by the squares of the frequency coefficients. The frequency coefficients of the half-Nyquist filter obtained for K=2,3 and 4 are given in Table1.

K	H0	H1	H2	H3
2	1	0.7071	--	--
3	1	0.9114	0.4114	--
4	1	0.9717	0.7071	0.2351

Table 1. Frequency domain prototype filter coefficients

In the frequency domain, the filter response consists of 2K-1 pulses, as shown in Fig.3.5 for K=4. The continuous frequency response, also shown in Fig.3.5, is obtained from the frequency coefficients through the interpolation formula for sampled signals which yields

$$H(f) = \sum_{k=-(K-1)}^{K-1} H_k \frac{\sin(\Pi(f-k/MK)MK)}{Mk\sin(\Pi(f-k/MK))} \qquad \text{--(19)}$$

The out-of-band ripples have nearly disappeared and a highly selective filter has been obtained.

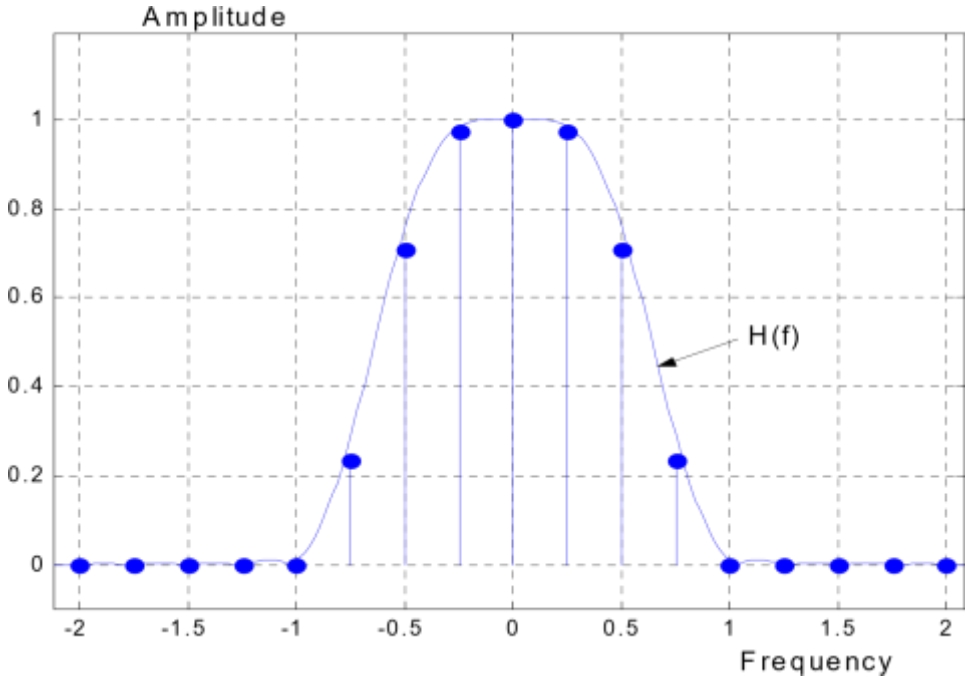

Fig.3.5. Prototype filter frequency coefficients and frequency response for K=4.

The impulse response h(t) of the filter is given by the inverse Fourier transform of the pulse frequency response, which is

$$h(t) = 1 + 2\sum_{k=1}^{k-1} H_k \cos(2\pi kt/KT) \quad \text{-(20)}$$

It is shown in fig.3.6 for the filter length L=1024, the number of sub-channels M=256 and K=4.

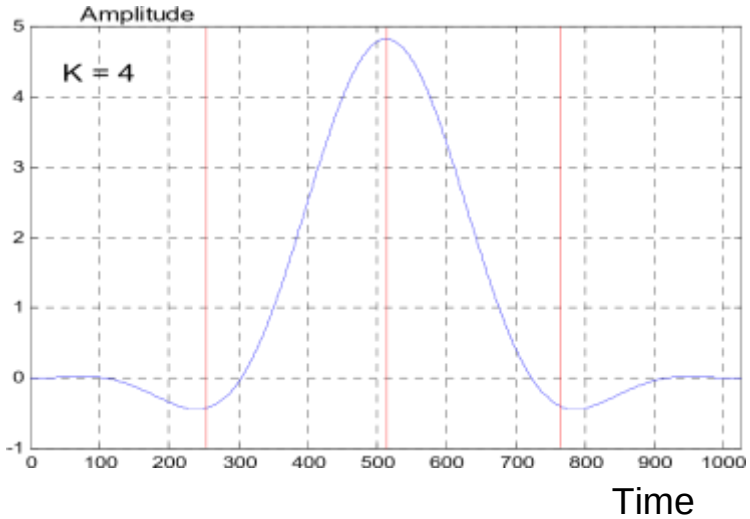

Fig.3.6. Impulse response of the prototype filter for overlapping factor K=4.

Once the prototype filter has been designed, the filter bank is obtained by the frequency shifts k/M, as in the FFT case. The filter with index k is obtained by multiplying the prototype filter coefficients by $e^{j2\pi k/M}$, as mentioned in section 2 for the FFT. A section of the filter bank derived in that manner is shown in Fig.3.7. The sub-channel index corresponds to the frequency axis and the sub-carrier spacing is unity. A key observation is that the sub-channels with even index (odd index) do not overlap. This has a great impact on systems as will be emphasized below. In fact, a particular sub-channel overlaps in frequency with its neighbours only.

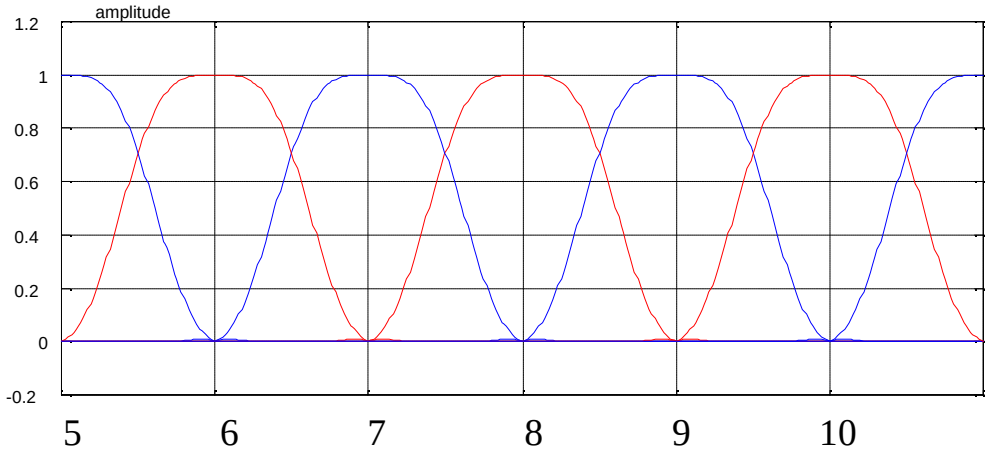

Fig.3.7. Section of a filter bank based on the prototype with K=4

The intersub-channel interference frequency response is important because it determines the modulation scheme.
As illustrated in Fig.3.7, for a given sub-channel, the receiver filter of this sub-channel overlaps with the transmitter filter of the neighbouring sub-channel. Considering the frequency coefficients of two neighbouring sub-

channels, the overlap concerns K-1 coefficients and the frequency coefficients of the interference filter are

$$G_k = H_k H_{K-k};\ k = 1,.....,K-1$$

The set of coefficients is symmetrical and for K = 4

$$G_1 = 0.228553 = G_3;\ G_2 = 0.5$$

As previously mentioned, the interference frequency response is derived with the help of the interpolation formula which yields

$$G(f) = \sum_{k=-(K-1)}^{K-1} G_k \frac{\sin(\Pi(f-k/MK)MK)}{Mk\sin(\Pi(f-k/MK))} \quad --(21)$$

The frequency response of the interference filter is shown in Fig.3.8 for K = 4. In the time domain, the interference filter impulse response is given by the inverse Fourier transform

$$g(t) = [\ G_2 + 2G_1 \cos(2\pi\ (t/KT))\ ]\ e^{j2\pi\ t/2T} \quad --(22)$$

This is a crucial result, which determines the type of modulation which must be used to dodge interference. The factor $e^{2T} = \cos(\pi t/T) + j\sin(\pi t/T)$ reflects the symmetry of the frequency coefficients and, due to this factor, the imaginary part of g(t) crosses the zero axis at the integer multiples of the symbol period T while the real part crosses the zero axis at the odd multiples of T/2. The zero crossings are interleaved and it is the basis for the OQAM modulation presented in a later section.

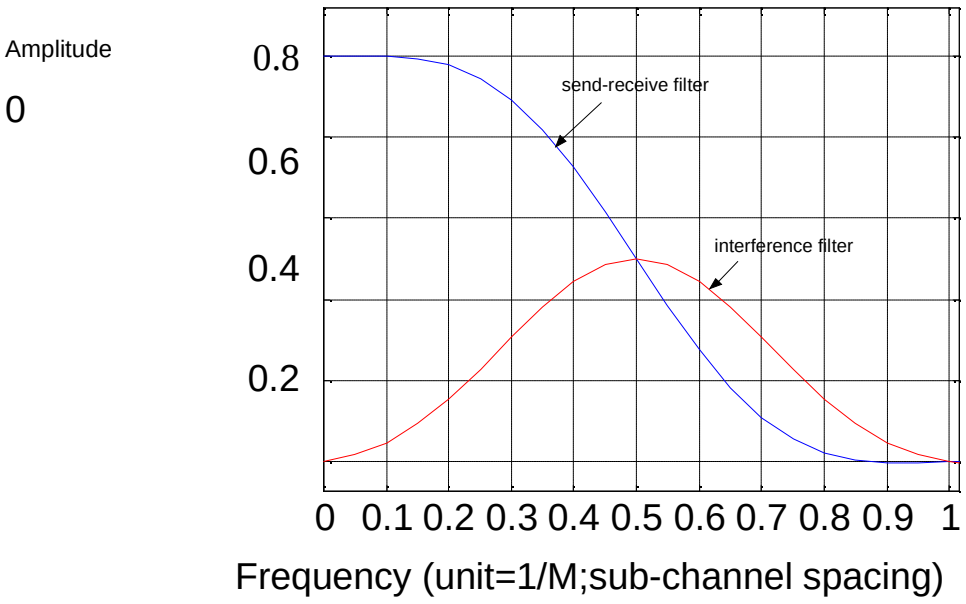

Fig.3.8. Frequency responses of the sub-channel filter and interference filter

Now, considering the complete system, the frequency coefficients of the transmitter-receiver filter are the squares of those of the prototype. The corresponding responses are given by

$$h(t) = 1 + 2\sum_{k=1}^{k-1} H_k \cos(2\pi kt/KT)$$

$$H2(f) = \sum_{k=-(K-1)}^{K-1} H2_k \frac{\sin(\Pi(f-k/MK)MK)}{Mk\sin(\Pi(f-k/MK))} \qquad \text{--(23)}$$

This is a Nyquist filter and its frequency response is shown in Fig.8 for K = 4. An important parameter related to the prototype filter design is the "background noise" power. Actually, it is the residual interference power due to the non-orthogonality of the carriers beyond the neighbouring sub-channels. It is measured, for example, by loading all the sub-channels but one with uncorrelated unit power signals and measuring the signal power in the unloaded sub-channel. The values σ^2 obtained for different overlapping factors K are reported in the last column of Table 1. The parameter is important for system design because it impacts bit loading and spectrum sensing. Once a design is available comes the implementation.

3.3 Extending the FFT to implement the filter bank

The simple scheme depicted in Fig.1 can be adapted to implement the filter bank, it is just sufficient to extend the iFFT and the FFT. In section 1, a data element is applied to one input of the iFFT and it modulates one carrier. In a filter bank with overlapping factor K, as shown in Fig.3.5, a data element modulates 2K-1 carriers. Thus, the filter bank in the transmitter can be implemented as follows

- an iFFT of size KM is used, to generate all the necessary carriers,
- a particular data element $d_i(mM)$, after multiplication by the filter frequency coefficients, is fed to the 2K-1 inputs of the iFFT with indices $(i-1)K+1,\ldots\ldots,(i+1)K-1$. Practically, the data element is spread over several iFFT inputs and the operation can be called "weighted frequency spreading".

For each set of input data, the output of the iFFT is a block of KM samples and, since the symbol rate is 1/M, K consecutive iFFT outputs overlap in

the time domain. Therefore, the filter bank output is provided by an overlap and sum operation, as shown in Fig.3.9.

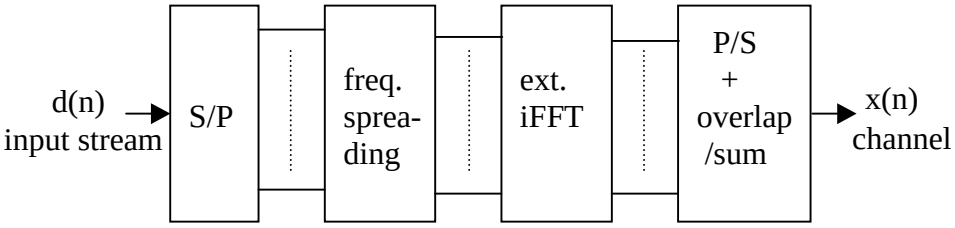

Fig.3.9. Principle of the filter bank based transmitter implemented with iFFT extension

Details of the implementation are given in Fig.3.10 for the overlapping factor K =4. The figure

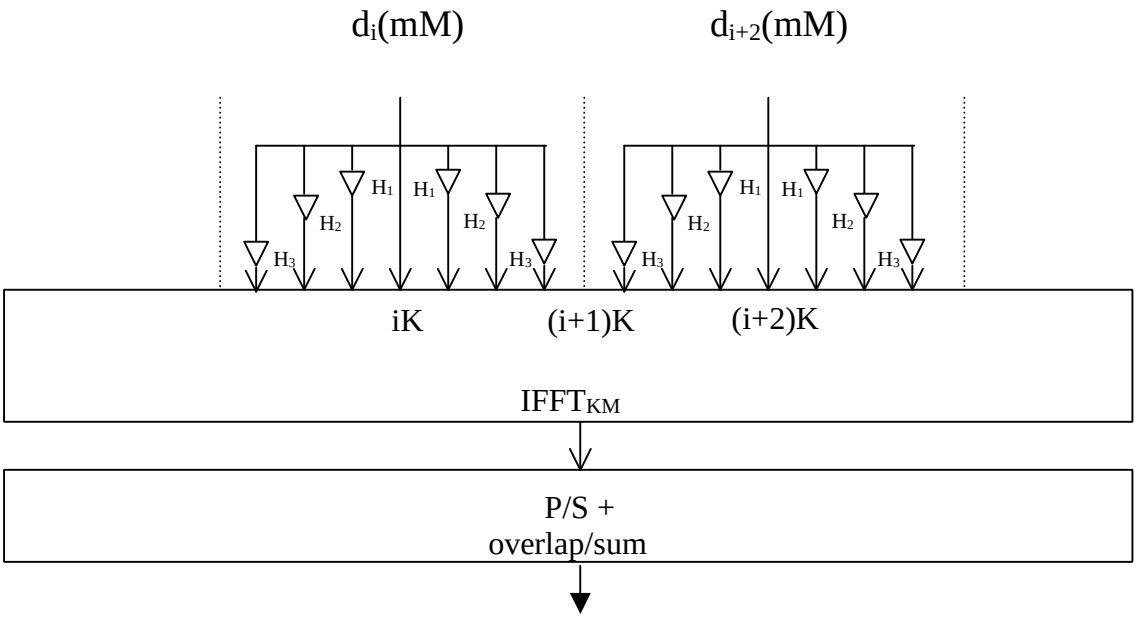

x(n) Fig.3.10. Weighted frequency spreading and extended iFFT

shows that the sub-channels with indices i and i+2 are separated and do not overlap. On the contrary, sub-channel i+1 overlaps with both and orthogonality is necessary. It is provided by using real inputs of the iFFT for i and i+2, and imaginary inputs for i+1, or the inverse.

The implementation of the receiver is based on an extended FFT, of size KM. In that case, the FFT input blocks overlap, it is the classical sliding window situation. At the output of the FFT, the data elements are recovered with the help of a weighted despreading operation whose details are given in Fig.11. In fact, the data recovery rests on the following property of the frequency coefficients of the Nyquist filter

$$\frac{1}{k}\sum_{k=-(\kappa+1)}^{k-1} 1\, Hk^2 \quad = 1 \qquad \text{--(24)}$$

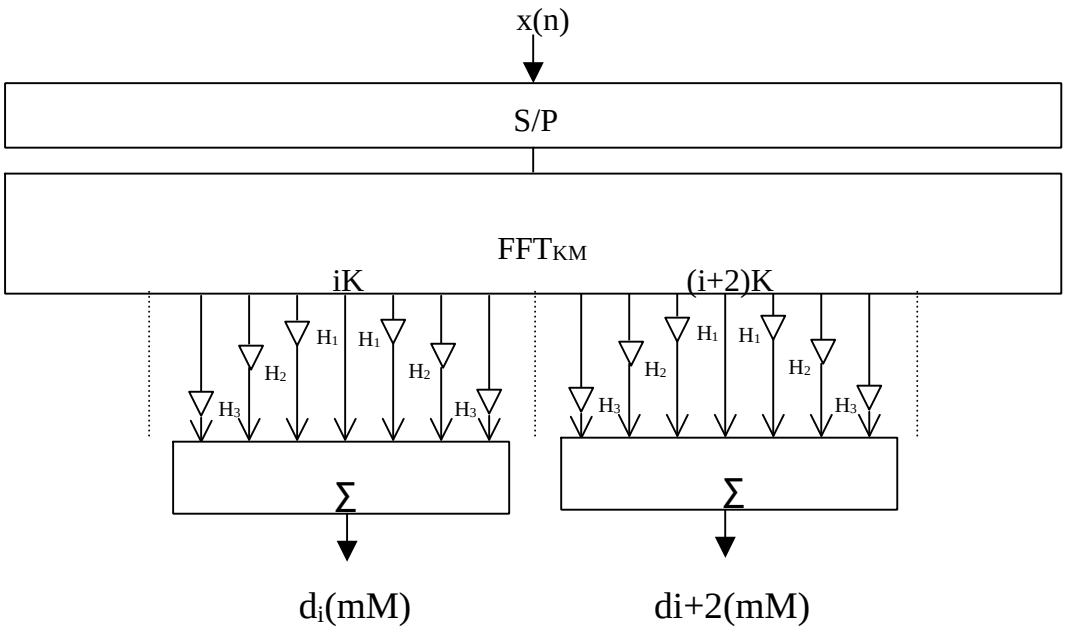

Fig.3.11. Extended FFT and weighted despreading in the filter bank-based receiver

When the transmitter and the receiver are connected back to back, the delay of the system is KM transmitted samples, or K multicarrier symbols.

A remarkable feature of the scheme presented is its simplicity : it is just the scheme of Fig.3.1 completed by minor operations before and after the iFFT and the FFT. In fact, the key difference is the computational complexity, due to the size of the FFT which is increased from M to KM and an issue is how to reduce this complexity.

Due to the overlapping in the time domain of the iFFT outputs and FFT inputs, a significant amount of redundancy is present in the computations.

An efficient approach to reduce this redundancy is the so-called PPN-FFT scheme.

3.4 PPN-FFT to reduce computational complexity

A frequency domain vision of filter banks has been presented in the previous section. In this section, the equivalent time domain vision is described, with the objective to reduce the computational complexity. In fact, it will be shown that the size of the FFT can be kept to M, as in Fig.3.1, but some additional processing is needed, called polyphase network (PPN).
In the time domain, the prototype filter is defined by a set of coefficients and the relationship between input and output sequences, which is

$$y(n) = \sum_{i=0}^{L-1} h_i x\,(n-i) \qquad \text{--(25)}$$

The filter impulse response, of length L , is the sequence of coefficients h_i ($0 \le i \le L-1$) and the frequency response is expressed by

$$H(f) = \sum_{i=0}^{L-1} h_i e^{-i 2\pi i f} \qquad \text{-(26)}$$

where the sampling frequency is assumed to be unity.
The filter has linear phase if the coefficients are symmetrical and, in this case, the delay is

$$\tau = L-1/2$$

In digital signal processing, and particularly in digital filtering, it is customary to use the Z-transfer function, which generalizes the frequency response and is defined by

$$H(z) = \sum_{i=0}^{L-1} h_i z^{-1} \qquad \text{--(27)}$$

The filter frequency response is the restriction of the Z-transfer function to the unit circle, i.e. it is obtained by letting $Z = e^{j2\pi f}$.
Now, if we assume, as in the previous section, that the filter length is a product of two factors, L=K.M, the sequence of filter coefficients can be

decomposed into M interleaved sequences of K coefficients and the Z-transfer function can be expressed as a double summation

$$H(z) = \sum_{p=0}^{p-1} H_P(z^M) Z^{-p}$$

$$H_P(z^m) = \sum_{k=0}^{k-1} h_{kM+P} z^{-kM} \qquad \text{--(28)}$$

It turns out that each individual filter element, $H_p(Z^M)$, has the frequency response of a phase shifter, hence the name of polyphase decomposition, and polyphase network for the complete set.

Now, turning to the filter bank in the transmitter, which is generated by shifting the response of the prototype filter on the frequency axis, a global Z-transfer function can be derive

Shifting the frequency response of the filter *H(f)* by 1/M on the frequency axis leads to the function.

$$B_i(f) = H(f - \frac{1}{M}) = \sum_{i=0}^{I-1} h_i e^{-j2\pi i(f-1/M)}$$

The corresponding Z-transfer function is

$$B_i(Z) = \sum_{i=0}^{I-1} h_i c^{j2\pi i/M} Z^{-i} \qquad \text{--(29)}$$

and it is expressed in terms of the polyphase decomposition by

$$B_i(Z) = \sum_{p=0}^{M-1} e^{j\frac{2\pi}{M}p} Z^{-p} H_p(Z^M) \qquad \text{--(30)}$$

The key point here is that the functions $H_p(Z^M)$ are not affected by the frequency shift. Then, considering all the shifts by multiples of 1/M and the associated filters, and letting $W = e^{-j2\pi/M}$, a matrix equation is obtained

$$\begin{bmatrix} B_0(Z) \\ B_1(Z) \\ . \\ . \\ B_{M-1}(Z) \end{bmatrix} = \begin{bmatrix} 1 & 1 & . & . & 1 \\ 1 & W^{-1} & . & . & W^{-M+1} \\ . & . & . & . & . \\ . & . & . & . & . \\ 1 & W^{-M+1} & . & . & W^{-(M-1)^2} \end{bmatrix} \begin{bmatrix} H_0(Z^M) \\ Z^{-1} H_1(Z^M) \\ . \\ . \\ Z^{-(M-1)} H_{M-1}(Z^M) \end{bmatrix}$$

The square matrix is the matrix of the inverse discrete Fourier transform (iDFT) and all the filters in the bank have the same filter elements $H_p(Z^M)$. In the implementation, the transmitter output is the sum of the outputs of the filters of the bank. Thus, the processing associated with the filter elements $H_p(Z^M)$ can be carried out after the summation which is performed by the iDFT. Finally, the structure for the implementation of the filter bank in the transmitter is shown in Fig.3.12.

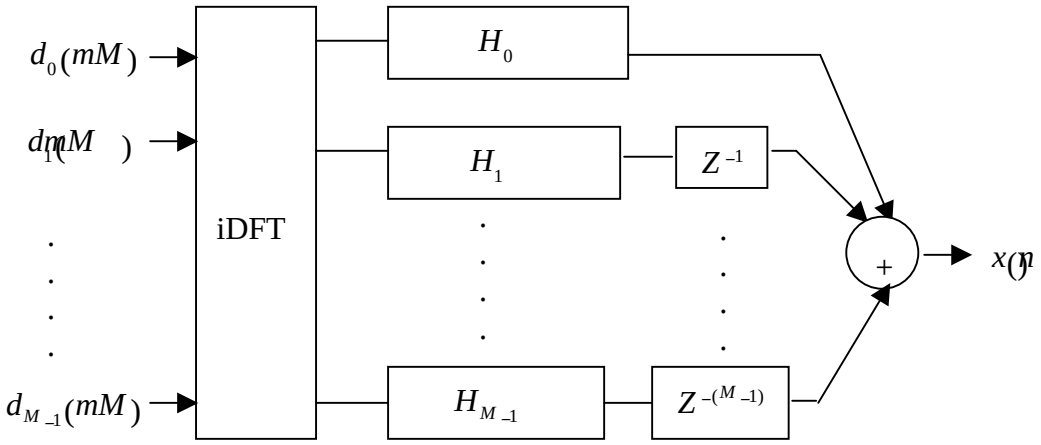

Fig.3.12 PPN-iFFT implementation of the transmitter filter bank

The same scheme applies to the filter bank in the receiver. The difference is that the frequency shifts are multiples of –1/M and the discrete Fourier transform (DFT) replaces the iFFT. In fact, for each sub-channel, the signal of interest is shifted around the frequency origin and filtered. Again, the filter elements are the same for all the filters in the bank and, since it is the sum of the sub-channel signals which is received, the processing can be common and the separation of the signals can take place afterwards, with the help of the DFT.

The block diagram of the transmission system is shown in Fig.3.13. Of course, in practice, the size of the DFT is a power of two and the fast Fourier transform algorithm is implemented. The difference in structure between figures 3.1 and 3.13 is just the PPN in the transmitter and the receiver. Note that the system delay is K multicarrier symbol periods, due to the delay of the prototype filter in the transmit and receive filter banks.

In terms of complexity, each section of the PPN has K multiplications, as shown in Fig.3.14 for K=4, and the complete PPN requires KM multiplications, which is less than the iFFT, as soon as the number M of sub-channels becomes large.

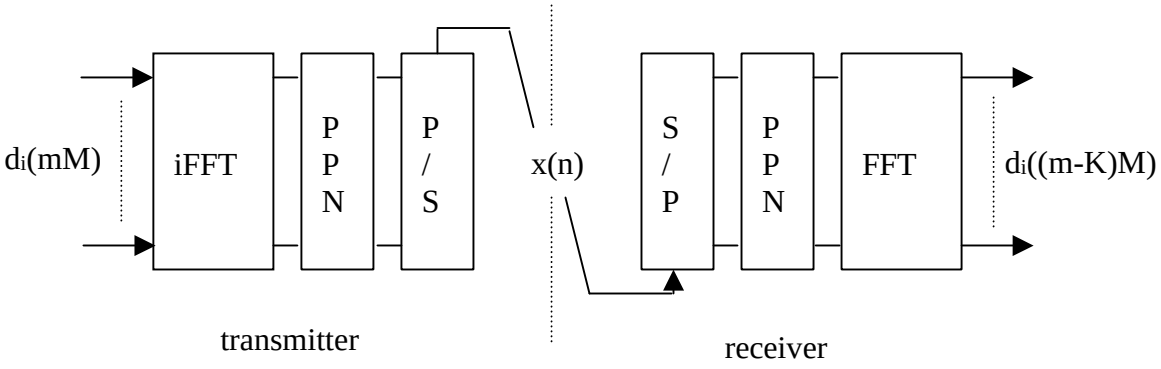

Fig.3.13. Transmission system using the PPN-FFT schem

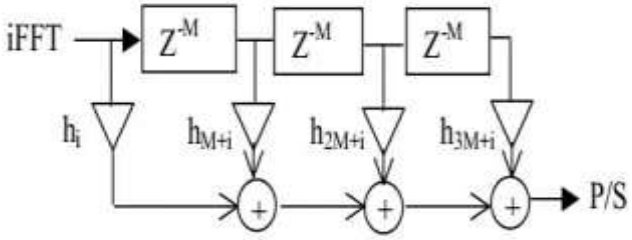

Fig.3.14. A section of the PPN in the transmitter (K=4)

The transmitter can generate a real sequence, with almost the same computational complexity. The iFFT size has to be doubled and every input data element di(mM) is applied to two symmetrical inputs. Then, the iFFT output is real and, since the PPN coefficients are real, the transmitter output is real. The receiver can process real signals, with similar changes.

3.5 OQAM modulation

In FBMC systems, any kind of modulation can be used whenever the sub-channels are separated. For example, if only the sub-channels with even

(odd) index are exploited, there is no overlap and QAM modulation can be employed. However, if full speed is seeked, all the sub-channels must be exploited and a specific modulation is needed to cope with the frequency domain overlapping of the neighbouring sub-channels.

Two important aspects of the transmission systems have been pointed out in sections 3 and 4

1) due to the overlapping of neighbouring sub-channels, orthogonality is needed. It is achieved by using the real part of the iFFT inputs with even index and the imaginary part of the iFFT inputs with odd index. But this implies a reduction of the capacity by the factor 2. In fact, full capacity can be restored with the second aspect.

2) Due to the symmetry of the transmitter and receiver filters and the fact that they are identical, the imaginary part of the impulse response of the sub-channel interference filter crosses the time axis at the integer multiples of the symbol period and the real part crosses the time axis at the odd multiples of half the symbol period. The time axis crossings are interleaved, as explained at the end of section 3.

Then, the strategy to reach full capacity is the following: double the symbol rate and, for each sub-channel, use alternatively the real and the imaginary part of the iFFT. This way, the real and the imaginary part of a complex data symbol are not transmitted simultaneously as in OFDM, but the imaginary part is delayed by half the symbol duration. The scheme is fully explained by considering the impulse response of the transmitter-receiver cascade.

The most significant part of the impulse response of the transmission system is given in Table 2, for the prototype filter with overlapping factor K = 4. The time unit is half the inverse of the sub-channel spacing, that is T/2. It is observed that in sub-channel with index “i”, all the terms are real and the Nyquist criterion is reflected by the zeros. In sub-channels “i-1” and “i+1”, real and imaginary terms alternate, the terms which are simultaneous to the reference term “1” being real. Therefore, from this table, it appears that

- data can be transmitted on the real part of sub-channel i at sub-channel spacing rate,
- data can be transmitted on the imaginary part of sub-channel i at sub-channel spacing rate and with a unit time shift,

- the same scheme can be applied for transmission in the neighbouring sub-channels i+1 and i-1, provided the real and imaginary parts are interchanged.

This is the so-called offset quadrature amplitude modulation (OQAM) and the term ‘offset’ reflects the time shift of half the inverse of the sub-channel spacing between the real part and the imaginary part of a complex symbol. Note that this type of modulation is used in single carrier systems, to improve the peak factor. In the present multicarrier context the throughput rate is the same as with QAM modulation, employed for example in OFDM systems, but without the guard time.

As concerns implementation, the extended FFT approach of section 4 can be used. The rate is doubled and, in the transmitter, consecutive blocks of M output samples overlap and the overlapping parts with M/2 samples are added. In the receiver, the FFT window slides by M/2 samples instead of M samples. The PPN-FFT approach requires two chains, or a single FFT running at double rate and two PPN devices, as shown in Fig.3.15 for the transmitter. As mentioned above, the blocks of M output samples coming out of PPN1 and PPN2 overlap by M/2 samples and an addition is introduced, as shown in the figure.

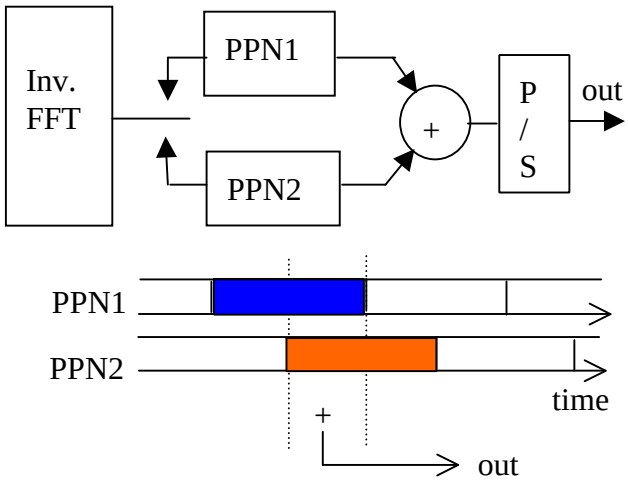

Fig.3.15. An OQAM transmitter using the iFFT-PPN scheme

At this stage, an important aspect of the OQAM modulation is worth emphasizing, because it will impact some of the functions of the transmission system and, particularly, some applications of the MIMO concept. Let us consider Fig.3.13 and the output of the FFT in the receiver. Using the notations of Table 2, the signal $y_i(p)$ coming out of sub-channel

i at time p contains the useful data element either in its real or imaginary part, and the other part is an interference term determined by the impulse response as in Table 2. Assuming the data element is in the real part, the output signal is expressed by

$$y_i(p) = d_i(p) + ju_i(p) \qquad \text{--(31)}$$

In this expression, $d_i(p)$ is the desired data element and $u_i(p)$ is an interference sample expressed in terms of the impulse response coefficients and the neighbouring data elements by

$$u_i(P) = \sum_{l=-1}^{1} \sum_{k=-(2k-1)}^{2k-1} c_{lk} d_{i+1}(p-k) \quad ; k, l \,! = 0$$

The coefficients c_{lk} involved in the above expression have the following property

$$\sum_{l=-1}^{1} \sum_{2k-1}^{2k-1} |c_k|^2 = 1 \quad ; \text{k,l}\neq 0 \qquad \text{--(32)}$$

Therefore, the power of the interference terms equals the power of the data elements, assumed statistically independent. The histogram of their amplitudes is shown in Fig.16 for binary data and K=4.

The interference terms and their amplitude distribution have an impact on some of the system functions, such as pilot detection and MIMO processing.

CHAPTER 4
TRANSMITTER & RECEIVER

4.1 FBMC TRANSMITTER BLOCK DIAGRAM:

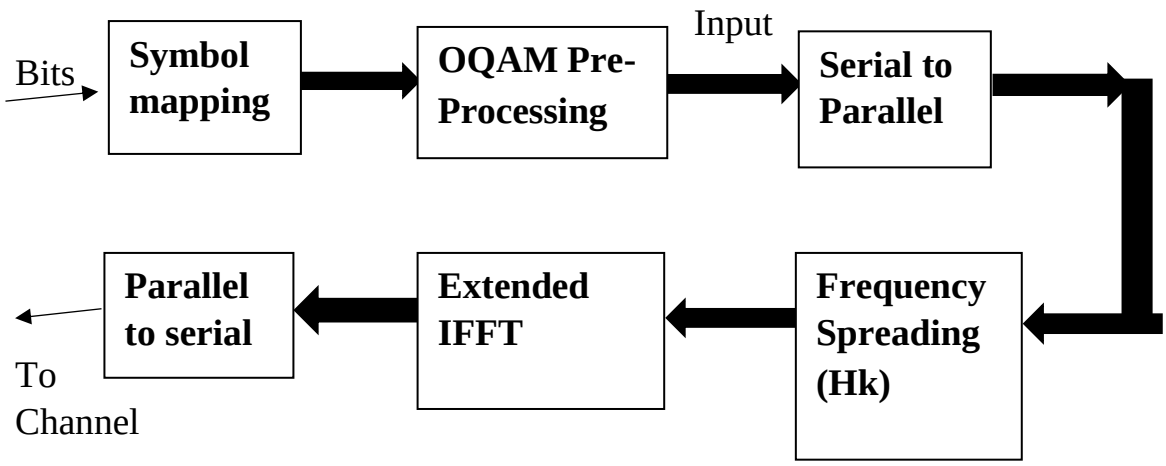

The order of the prototype filter can be set to 2K-1, where K is the overlapping factor.

The number of multicarrier symbols that overlap in the time domain is K, which is the ratio of filter impulse response duration to multicarrier symbol period T. The incoming data bits can be turned into symbols using symbol mapping. In FBMC, OQAM (Offset Quadrature Amplitude Modulation) transmits the imaginary component of the sub channel interference filter's impulse response across the time axis at integer multiples of symbol period, while the real part crosses at odd multiples of half the symbol period. Half of the symbol duration T will be delayed between the real and imaginary parts. To acquire the entire channel capacity, OQAM uses orthogonality between the subchannels. This orthogonality can be obtained without needing a cyclic prefix like OFDM by employing the PYDYAS filter and OQAM. After that, the bits are transformed from serial to parallel. In FFT, a data element can be modulated with just one carrier, but in extended IFFT, it will be modulated with 2K-1 carriers. As a result, the filter bank in the transmitter is set up as follows. We are utilising an IFFT of length KM in this case. The IFFT output is a block of KM samples with a symbol rate of 1/M for each data input, and K successive IFFT outputs overlap in time domain. The data element will be sent into the IFFT's 2K-1 input, i.e.,

the data element will be spread across several IFFT inputs, and the operation will be referred to as "weighted frequency spectrum." To achieve symmetry, the Nyquist filter is separated into two pieces. Half of the Nyquist prototype transmitter filter and half of the Nyquist prototype receiver filter are cascaded together. The filter's frequency coefficients for k=2,3,4

K	H0	H1	H2	H3
2	1	0.7071	--	--
3	1	0.9114	0.4114	--
4	1	0.9717	0.7071	0.2351

The filter order can be set to 2K-1, with K denoting the overlapping factor. The frequency response equation for the filter should be

$$H(f) = \sum_{k=-(K-1)}^{K-1} H_k \frac{sin(\Pi(f-k/MK)MK)}{Mk\, sin(\Pi(f-k/MK))}$$

We can eliminate out of band ripples by creating a good prototype filter (M=number of sub channels). h(t) is the filter impulse response is

$$h(t) = 1 + 2\sum_{k=1}^{k-1} H_k\, cos(2\pi kt/KT)$$

By shifting the prototype filter by k/M frequency shifts, the filter bank is created.

4.2 FBMC RECEIVER BLOCK DIAGRAM:

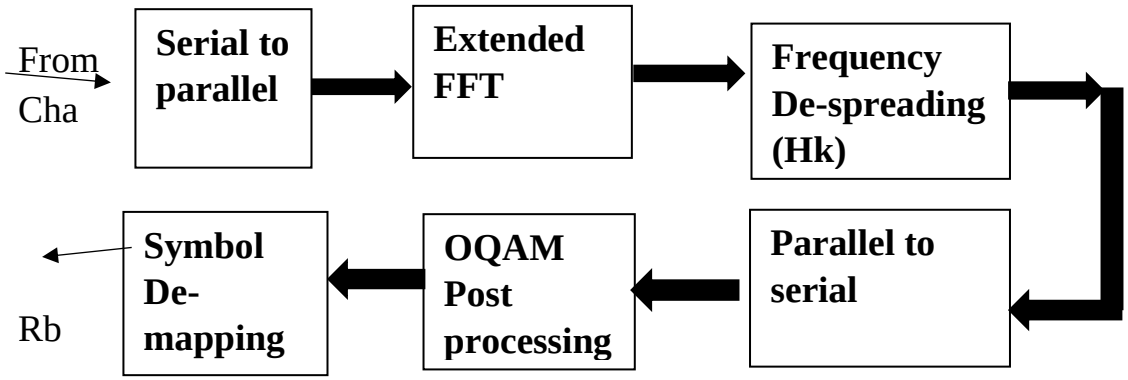

Rb- Received bits cha-channel

In this case, Half of the Nyquist prototype transmitter filter and half of the Nyquist prototype receiver filter are cascaded together. After the symbol sequences have been changed from parallel to serial in the transmitter, the

channel can be used. The data bits are received from the channel at the receiver end, and the demodulation process is converted from serial to parallel. The FBMC approach employs a network of filters on both sides of the receiving end, including an analysing filter and a fast Fourier transform (FFT) demodulator. A data element can be modulated with a single carrier in FFT, but in extended FFT, a data element is modified with N*K length FFT symbols overlapped with a delay of N/2, where N is the number of subcarriers and T is the time spacing between them. The frequency De-spreading technique is used in this FBMC approach. Data symbols' real and imaginary parts are not received, and the imaginary component is delayed by half the symbol's time. The input data symbols are then transformed back to parallel from serial. The demultiplexing phases in FBMC-OQAM post processing are where FBMC-OQAM accomplishes the real to complex number conversion. where down sampling takes place and matching filtering is used to merge the real and imaginary parts of symbols to produce the received data symbols

The resultant symbols are then received, and demapping is performed, in which the symbols are translated to resultant bits, allowing the bit error to be calculated. As a result, at the receiver end, the resulting bits are retrieved.

CHAPTER 5
SIMULATION RESULTS

5.1 Power spectral density of OFDM and FBMC:

the Power Spectral Density (PSD) of OFDM and FBMC. The PSD of OFDM is plotted, that has a large side lobe which gives high Out of Band leakage, and where as in PSD of FBMC is designed in order to get the low Out of Band leakage. Using the PSD we can compute the BER versus SNR and PAPR for OFDM and FBMC. There are a more side lobes in OFDM which makes the minimum utilization of assigned spectrum which leads the non-progressive spectral efficiency. Thus it requires more power in OFDM.

The first side lobe of OFDM is almost -30dB on both side and the first side lobe of FBMC is almost -100 dB Thus there is a remarkable difference in the two modulation techniques. Hence there is an interesting observation in OFDM and FBMC side lobe power reduces approximately -70dB on both sides. Therefore we can see that the reduced side lobes in FBMC, this makes the maximum utilization of assigned spectrum which leads the progressive spectral efficiency. Thus it requires less power.

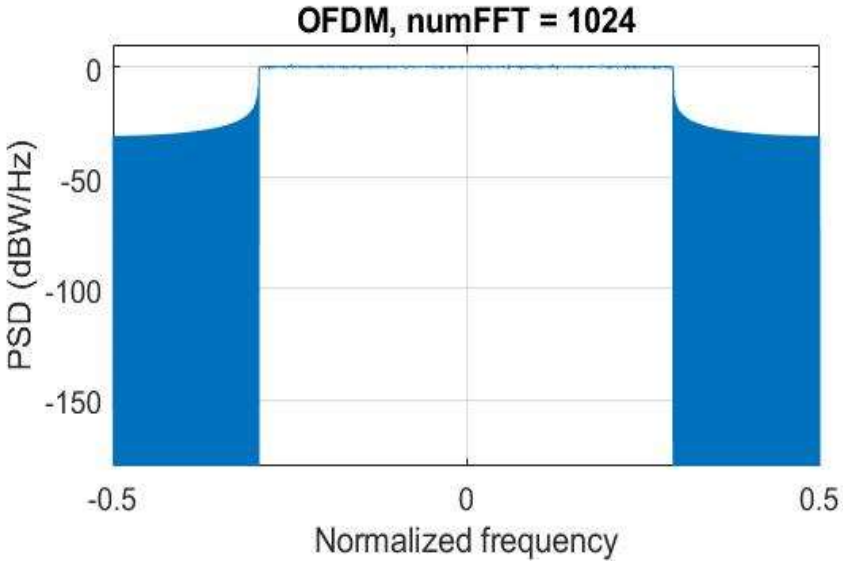

PSD of OFDM

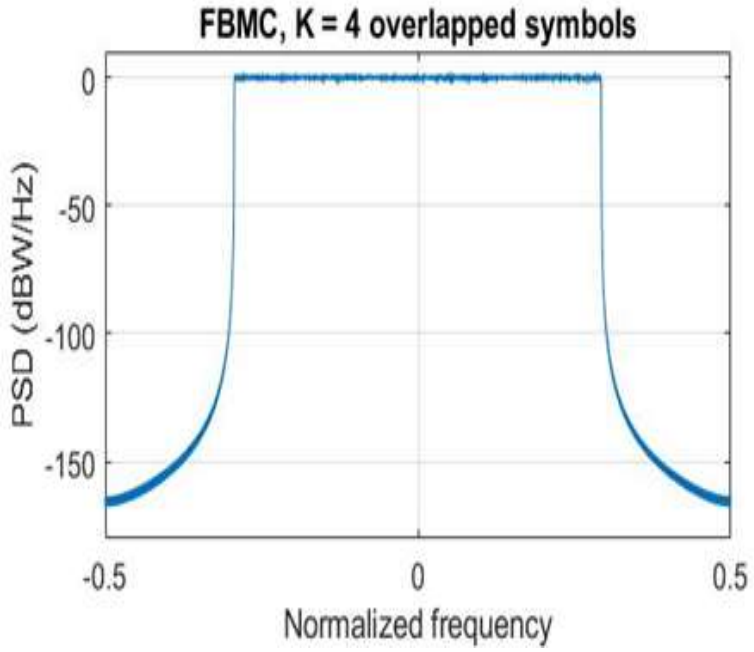

PSD of FBMC

5.2 Power spectral density of FBMC using different filters:

Using various filters, the power spectral density of FBMC is shown in the diagram above. High pass, Chebyshev, and Butterworth filters are used here. When comparing the power spectral density FBMC using these filters, the first sidelobe of the high pass filter is almost at -30db, the first sidelobe of the Chebyshev filter is at -50db, and the first sidelobe of the Butterworth filter is at -60db. We previously knew that as the size of the side lobe PSD lowers, the quantity of necessary power falls as well. By comparing all of these filters, we can use the Butterworth filter to lower the necessary power in FBMC.

When comparing the Chebyshev and high pass filters to the Butterworth filter, we notice that the distortion is higher Chebyshev and high pass compared to Butterworth filter. The Butterworth filter, in comparison to high pass and Chebyshev filters, is more useful. Now we compare the Butterworth filter to the PHYDYAS filter, with the first sidelobe in the Butterworth filter being -60db and the first sidelobe in the PHYDYAS filter being -95db. The difference indicates that the sidelobes are almost minimize -35db on both sides. As a result, when comparing the PHYDYAS filter to the Butterworth filter, the needed power in FBMC using PHYDYAS will be lower. This is why the PHYDYAS filter was chosen as a filter in the FBMC for 5G communication.

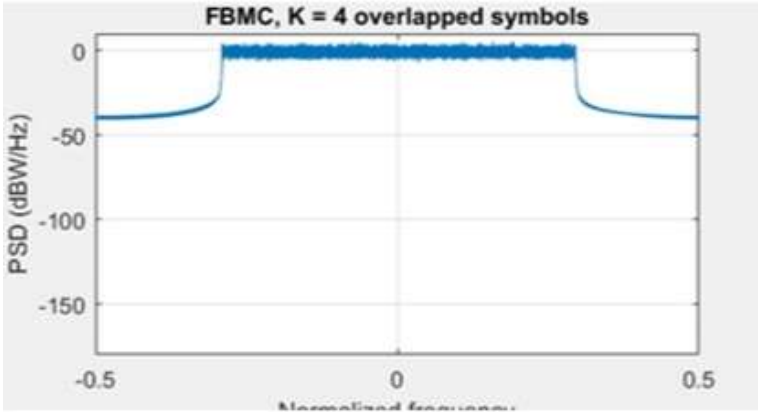

USING HIGH PASS FILTER

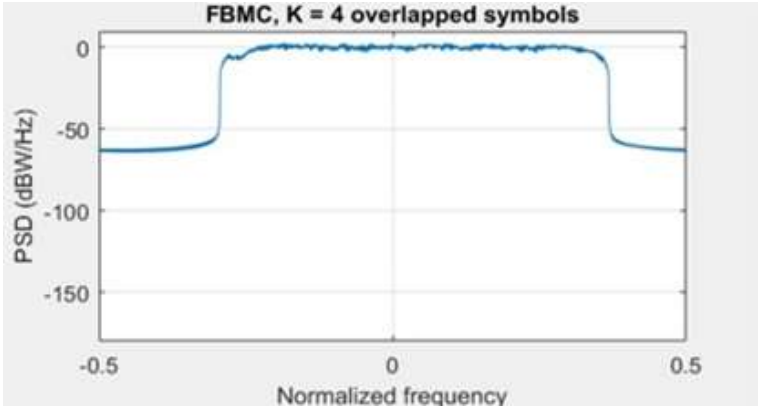

USING BUTTERWORTH FILTER

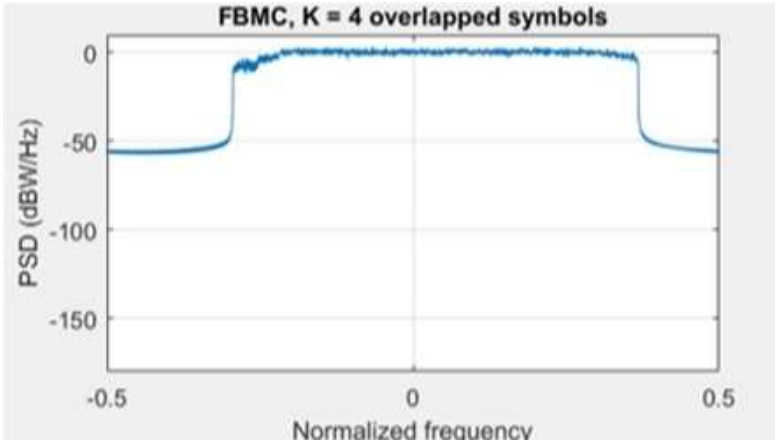

USING CHEBYSHEV FILTER

5.3 PAPR (Peak to average power ratio) in OFDM and FBMC:

The Peak to average power ratio is the relation between the maximum power of a sample in a given OFDM transmit symbol divided by the average power of that OFDM symbol. PAPR is ratio of peak power to the average power of a signal (expressed in dB).

PAPR occurs when in a multi carrier system the different sub-carriers are out of phase with each other. At each instant they are different phase values. When all the points achieve the maximum value simultaneously; this will cause the output envelope to suddenly shoot up which causes a peak in the output voltage.

In any communication system, the linear power amplifier is used in transmitter side and the operating point to be in linear region for a linear power amplifier.

The operating point moves to the saturation region due to high PAPR. So to keep the operating point in linear region, the dynamic range of the power amplifier should be increased which reduces the overall efficiency and increase in the cost of the power amplifier. Trade-off between efficiency and nonlinearity will be there, So in order to increase the efficiency of the power amplifier we need to reduce the PAPR value.

$PAPR= [\max\{|d[n]|^2\}/E\{|d[n]|^2\}\}$

Where |d[n]| is the amplitude of d[n] and E represents the expectation of the signal.

The PAPR value of 64 QAM in OFDM is 14, PAPR value of 64 QAM in FBMC is 10. Power is reduced in FBMC and FBMC has low PAPR compared to OFDM.

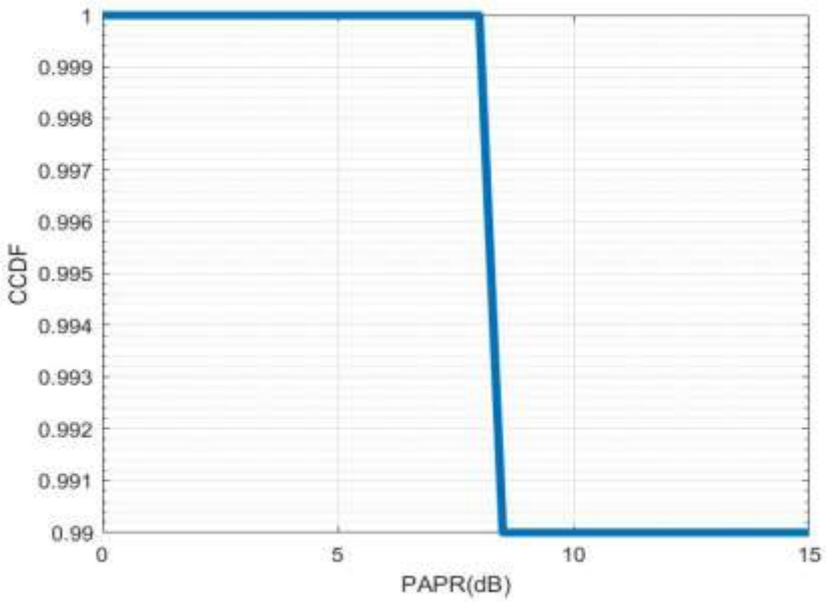

PAPR FOR FBMC

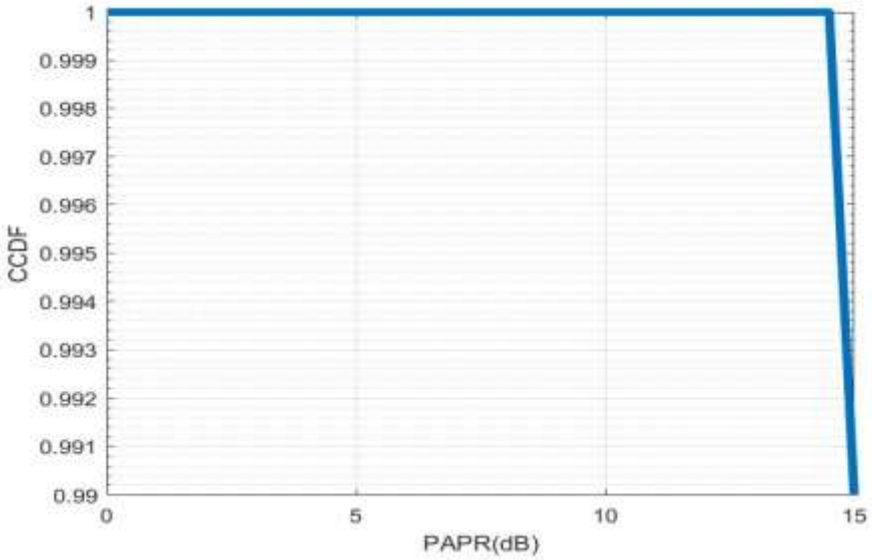

PAPR FOR OFDM

CHAPTER 6
CONCLUSION

This project shows how the FBMC in 5G communication is more advantageous when compared to OFDM in 4G communication. It also explains why Phydyas filter is used in FBMC. Here, transmitter and receiver are explained with the particular block diagrams. The order of the filter we choose as 2K-1 where K be the overlapping factor. For K=4 we get better spectral efficiency. In 4G we use Cyclic prefix which will requires high power to maintain and also more number of sidelobes will occur. This will cause minimized spectral efficiency, by using the banks of filter we will reduce the sidelobes so the required power will also be reduced. This will improve the spectral efficiency. In banks of filter due to sub-carrier filtering it shows a large filter delay, To reduce it we use OQAM processing. The main objective of this paper is to reduce the problems in 4G (OFDM) to migrate to 5G(FBMC). This will show by using PSD graphs and PAPR graphs of both FBMC and OFDM. In PSD of OFDM more number of sidelobes present, and also PSD of first sidelobe of OFDM is in high magnitude, So it requires more power while PSD of FBMC has less number of sidelobes. The PSD of first sidelobe of FBMC is less in magnitude and it requires less power when compared to OFDM. The required power reduced approximately -70 dB in FBMC compared to OFDM this can be achieved by using PHYDYAS filter instead of using other filters also FBMC has low PAPR compared to OFDM.

REFERENCES:

1. B. Saltzberg, “Performance of an efficient parallel data transmission system,” IEEE Trans. Com. Tech, vol. 15, COM-6, pp.805-811, Dec. 1967.

2. P. Siohan, and N. Lacaille, “Analysis of OFDM / OQAM Systems Based on the Filter bank Theory,” IEEE Global Telecommunications Conference, Rio de Janeiro, Brazil, December 1999.

3. Seung Hee Han; Jae Hong Lee, "An overview of peak-to-average power ratio reduction techniques for multicarrier transmission," Wireless Communications, IEEE , vol.12, no.2, pp.56,65, April 2005

4. T. Ihalainen, T. H. Stitz, M. Rinne, and M. Renfors, “Channel equalization in filter bank based multicarrier modulation for wireless communications,” EURASIP J. Adv. Signal Process., vol. 2007, Dec. 2007,Art. no. 49389.

5. B. Farhang Boroujeny, “ A square root Nyquist (M) filter design for digital communication systems,” IEEE Trans. Signal Process.,vol. 56.no.5,pp. 2127-2132,May 2008.

6. M. Bellanger, D. Le Ruyet, D. Roviras, M. Terré, J. Nossek, L. Baltar, et al., "FBMC physical layer: a primer," PHYDYAS, January, 2010.

7. Zs. Kollar and P. Horv´ath, “Modulation schemes for cognitive radio in white spaces,” Radioengineering, vol. 19, no. 4, pp. 511–517, Dec. 2010.

8. Zsolt Kollar, Lajos Varga, Balint Horvath, Peter Bakki, and Janos Bito, “Evaluation of Clipping Based Iterative PAPR Reduction Techniques for FBMC Systems”, Hindawi Publishing Corporation the Scientific World Journal Volume 2014, Article ID 841680, 12 pages.

9. J. Vihriala, N. Ermolova, E. Lahetkangas, O. Tirkkonen, and K. Pajukoski, “On the waveforms for 5G mobile broadband communications,” in Proc. IEEE VTC Spring, May 2015, pp. 1–5.
10. Arun kumar1, Shikha bharti, “Design and Performance analysis of OFDM and FBMC modulation”, Scientific Bulletin of the Electrical Engineering Faculty – Year 17 No.2 (37) ISSN 2286-2455.

11. Ronald Nissel, StefanSchwarz, and Markus Rupp, “Filter Bank Multicarrier Modulation Schemes for Future Mobile Communications”, IEEE journal on selected areas in communications, vol. 35, no. 8, August 2017

APPENDIX

```
s = rng(211);                    % Set RNG state for repeatability
numFFT = 1024;                   % Number of FFT points
numGuards = 212;                 % Guard bands on both sides
K = 4;                           % Overlapping symbols, one of 2, 3, or 4
numSymbols = 100;                % Simulation length in symbols
bitsPerSubCarrier = 2;           % 2: 4QAM, 4: 16QAM, 6: 64QAM, 8:
256QAM
snrdB = 12;                      % SNR in Db

% Prototype filter
switch K
   case 2
      HkOneSided = sqrt(2)/2;
   case 3
      HkOneSided = [0.911438 0.411438];
   case 4
      HkOneSided = [0.971960 sqrt(2)/2 0.235147];
   otherwise
      return
end

% Build symmetric filter
Hk = [fliplr(HkOneSided) 1 HkOneSided];

% Transmit-end processing
%   Initialize arrays
L = numFFT-2*numGuards;    % Number of complex symbols per OFDM
symbol
KF = K*numFFT;
KL = K*L;
dataSubCar = zeros(L, 1);
dataSubCarUp = zeros(KL, 1);
```

```
sumFBMCSpec = zeros(KF*2, 1);
sumOFDMSpec = zeros(numFFT*2, 1);

numBits = bitsPerSubCarrier*L/2;                % account for oversampling
by 2
inpData = zeros(numBits, numSymbols);
rxBits = zeros(numBits, numSymbols);
txSigAll = complex(zeros(KF, numSymbols));
symBuf = complex(zeros(2*KF, 1));

% Loop over symbols
for symIdx = 1:numSymbols

   % Generate mapped symbol data
   inpData(:, symIdx) = randi([0 1], numBits, 1);
   modData = qammod(inpData(:, symIdx), 2^bitsPerSubCarrier, ...
      'InputType', 'Bit', 'UnitAveragePower', true);

   % OQAM Modulator: alternate real and imaginary parts
   if rem(symIdx,2)==1     % Odd symbols
      dataSubCar(1:2:L) = real(modData);
      dataSubCar(2:2:L) = 1i*imag(modData);
   else                    % Even symbols
      dataSubCar(1:2:L) = 1i*imag(modData);
      dataSubCar(2:2:L) = real(modData);
   end

   % Upsample by K, pad with guards, and filter with the prototype filter
   dataSubCarUp(1:K:end) = dataSubCar;
   dataBitsUpPad       =       [zeros(numGuards*K,1);       dataSubCarUp;
zeros(numGuards*K,1)];
   X1 = filter(Hk, 1, dataBitsUpPad);
   % Remove 1/2 filter length delay
   X = [X1(K:end); zeros(K-1,1)];

   % Compute IFFT of length KF for the transmitted symbol
   txSymb = fftshift(ifft(X));
```

```
    % Transmitted signal is a sum of the delayed real, imag symbols
    symBuf = [symBuf(numFFT/2+1:end); complex(zeros(numFFT/2,1))];
    symBuf(KF+(1:KF)) = symBuf(KF+(1:KF)) + txSymb;

    % Compute power spectral density (PSD)
    currSym = complex(symBuf(1:KF));
    [specFBMC, fFBMC] = periodogram(currSym, hann(KF, 'periodic'),
KF*2, 1);
    sumFBMCSpec = sumFBMCSpec + specFBMC;

    % Store transmitted signals for all symbols
    txSigAll(:,symIdx) = currSym;
end

% Plot power spectral density
sumFBMCSpec                                                    =
sumFBMCSpec/mean(sumFBMCSpec(1+K+2*numGuards*K:end-
2*numGuards*K-K));
figure;
plot(fFBMC-0.5,10*log10(sumFBMCSpec));
grid on
axis([-0.5 0.5 -180 10]);
xlabel('Normalized frequency');
ylabel('PSD (dBW/Hz)')
title(['FBMC, K = ' num2str(K) ' overlapped symbols'])
set(gcf, 'Position', figposition([15 50 30 30]));
for symIdx = 1:numSymbols

    inpData2 = randi([0 1], bitsPerSubCarrier*L, 1);
    modData = qammod(inpData2, 2^bitsPerSubCarrier, ...
        'InputType', 'Bit', 'UnitAveragePower', true);

    symOFDM = [zeros(numGuards,1); modData; zeros(numGuards,1)];
    ifftOut = sqrt(numFFT).*ifft(ifftshift(symOFDM));

    [specOFDM,fOFDM] = periodogram(ifftOut, rectwin(length(ifftOut)),
...
        numFFT*2, 1, 'centered');
    sumOFDMSpec = sumOFDMSpec + specOFDM;
```

```
end

% Plot power spectral density (PSD) over all subcarriers
sumOFDMSpec                                                    =
sumOFDMSpec/mean(sumOFDMSpec(1+2*numGuards:end-
2*numGuards));
figure;
plot(fOFDM,10*log10(sumOFDMSpec));
grid on
axis([-0.5 0.5 -180 10]);
xlabel('Normalized frequency');
ylabel('PSD (dBW/Hz)')
title(['OFDM, numFFT = ' num2str(numFFT)])
set(gcf, 'Position', figposition([46 50 30 30]));
BER = comm.ErrorRate;

% Process symbol-wise
for symIdx = 1:numSymbols
   rxSig = txSigAll(:, symIdx);

   % Add WGN
   rxNsig = awgn(rxSig, snrdB, 'measured');

   % Perform FFT
   rxf = fft(fftshift(rxNsig));

   % Matched filtering with prototype filter
   rxfmf = filter(Hk, 1, rxf);
   % Remove K-1 delay elements
   rxfmf = [rxfmf(K:end); zeros(K-1,1)];
   % Remove guards
   rxfmfg = rxfmf(numGuards*K+1:end-numGuards*K);

   % OQAM post-processing
   %  Downsample by 2K, extract real and imaginary parts
   if rem(symIdx, 2)
      % Imaginary part is K samples after real one
      r1 = real(rxfmfg(1:2*K:end));
      r2 = imag(rxfmfg(K+1:2*K:end));
```

```
        rcomb = complex(r1, r2);
    else
        % Real part is K samples after imaginary one
        r1 = imag(rxfmfg(1:2*K:end));
        r2 = real(rxfmfg(K+1:2*K:end));
        rcomb = complex(r2, r1);
    end
    %  Normalize by the upsampling factor
    rcomb = (1/K)*rcomb;

    % De-mapper: Perform hard decision
    rxBits(:, symIdx) = qamdemod(rcomb, 2^bitsPerSubCarrier, ...
        'OutputType', 'bit', 'UnitAveragePower', true);
end

% Measure BER with appropriate delay
BER.ReceiveDelay = bitsPerSubCarrier*KL;
ber = BER(inpData(:), rxBits(:));

% Display Bit error
disp(['FBMC Reception for K = ' num2str(K) ', BER = ' num2str(ber(1)) ...
    ' at SNR = ' num2str(snrdB) ' dB'])
% Restore RNG state
rng(s);
% Compute peak-to-average-power ratio (PAPR)
PAPR = comm.CCDF('PAPROutputPort', true, 'PowerUnits', 'dBW');
[~,~,paprFBMC] = step (PAPR, txSymb);
disp(['Peak-to-Average-Power-Ratio (PAPR) for FBMC = '
num2str(paprFBMC) ' dB']);
[n, x] = hist(paprFBMC,0:0.5:30);

a=cumsum(n)/100;

figure;
plot(x,a,'LineWidth',4)
xlabel('PAPR(dB)')
ylabel('CDF')

grid on
```

```
% Compute peak-to-average-power ratio (PAPR)
PAPR2 = comm.CCDF('PAPROutputPort', true, 'PowerUnits', 'dBW');
[~,~,paprOFDM] = step(PAPR2,ifftOut);
disp(['Peak-to-Average-Power-Ratio (PAPR) for OFDM = '
num2str(paprOFDM) ' dB']);
[n1, y] = hist(paprOFDM,0:0.5:30);

b=cumsum(n1)/100;

figure;
plot(y,b,'LineWidth',4)
xlabel('PAPR(dB)')
ylabel('CDF')

grid on
```